CAIRT-PerReC

CAIRT Phase A Mission Performance and Requirement Consolidation (PerReC) Activity

ESA/ESTEC contract 4000136480/21/NL/LF CCN1

Deliverable D-24

Executive Summary Report

Björn-Martin Sinnhuber[1], Michael Höpfner[1], Cornelia Reimann Zumsprekel[1], Peter Preusse[2], Jan Kaumanns[2], Sebastian Rhode[2], Jörn Ungermann[2], Florian Voet[2], Bernd Funke[3], Stefan Bender[3], Quentin Errera[4], Jean-Christopher Lambert[4], Piera Raspollini[5], Pasquale Sellitto[6], Mona Kosary[6], Beatriz Monge-Sanz[7], Enzo Papandrea[8], Bianca Maria Dinelli[8], Kaley Walker[9], Patrick Sheese[9], Umberto Rizza[10], Tiziano Maestri[11], Stefano Corradini[12], Lorenzo Cassini[13], Arun Jo Mathew[14], Manyatt Pramitha[14], Han-Li Liu[15], Nicholas Pedatella[15], Simone Tilmes[15]

[1]**Karlsruhe Institute of Technology (KIT),** Hermann-von-Helmholtz-Platz 1, 76344 Eggenstein-Leopoldshafen, Germany
[2]**Forschungszentrum Jülich (FZJ),** Wilhelm-Johnen-Straße, 52428 Jülich, Germany
[3]**Instituto de Astrofísica de Andalucía (CSIC),** Gta. de la Astronomía, s/n, 18008 Granada, Spain
[4]**Royal Belgian Institute for Space Aeronomy (BIRA-IASB),** Ringlaan 3 Avenue Circulaire, 1180 Brussels, Belgium
[5]**IFAC/CNR** Via Madonna del Piano, 10 Sesto Fiorentino (Fi), Italy
[6]**Laboratoire Interuniversitaire des Systèmes Atmosphériques-Université Paris Est Créteil (LISA-UPEC),** 61, avenue du Général de Gaulle, 94010 Créteil Cedex, France
[7]**University of Oxford (Oxford),** Physics Department, Clarendon Laboratory, Parks Road, OX1 3PU, Oxford, UK
[8]**National Research Council of Italy-Institute of atmospheric sciences and climate (CNR-ISAC),** via P. Gobetti 101, 40129 Bologna, Italy
[9]**University of Toronto (UToronto),** Department of Physics, 60 St. George Street, Toronto, Ontario M5S 1A7 Canada
[10]**National Research Council of Italy-Institute of atmospheric sciences and climate (CNR-ISAC)**, strada Provinciale Lecce-Monteroni km.1.2, 73100 Lecce, Italy
[11]**Department of Physics and Astronomy "Augusto Righi", University of Bologna**, Viale Carlo Berti Pichat, 6/2, 40127 Bologna, Italy
[12]**National Institute of Geophysics and Volcanology, (INGV)**, via di Vigna Murata 605, 00143, Roma, Italy
[13]**School of Engineering of University of Basilicata (SI-UNIBAS)**, via dell'Ateneo Lucano 10, 85100, Potenza, Italy
[14]**School of Earth, Environmental and Sustainability Sciences, Indian Institute of Science Education and Research**, Thiruvananthapuram (IISER-TVM), Maruthamala PO, Vithura, Thiruvananthapuram - 695551, India
[15]**National Center for Atmospheric Research** (**NCAR**), 3090 Center Green Dr. Boulder, CO 80301, USA

Reference Number: DEL-24-CAIRT-PhAPerReC-1.2

Status: Final version

Version/revision: 1.2

Date: 22.01.2026

ESA Study Contract Report		
ESA Contract 4000136480/21/NL/LF CCN1	Title Executive Summary Report	Contractor Karlsruhe Institute of Technology

Abstract

This Executive Summary Report provides an overview of the CAIRT Phase A Mission Performance and Requirement Consolidation (PerReC) activities. PerReC reviewed the scientific objectives and societal impact of the CAIRT mission, including a consolidation of the observation requirements. Algorithm Theoretical Baseline Documents (ATBDs) were developed to describe the retrieval of primary Level-2 and Level-2b products. A scientific Workbench (SWB) was developed and used for a comprehensive performance assessment. PerReC provided a set of six impact studies, to show science closure of the primary mission objectives and impact in science applications. These included constraining the middle atmosphere circulation through age-of-air, consistent simulation of the dynamic driving and trace species impact of a sudden stratospheric warming, detection and characterization of geoengineering via stratospheric sulphur injection, Observing System Simulation Experiments for ozone and water vapour in the upper troposphere/lower stratosphere, an investigation of stratospheric composition for weather and climate prediction, and the detection of volcanic ash for aviation safety. Finally, an outlook and recommendations for future studies are given.

The work described in this report was done under ESA contract. Responsibility for the contents resides with the author(s) or organisation(s) that prepared it.

Names of authors

Björn-Martin Sinnhuber, Michael Höpfner, Cornelia Reimann Zumsprekel, Peter Preusse, Jan Kaumanns, Sebastian Rhode, Jörn Ungermann, Florian Voet, Bernd Funke, Stefan Bender, Quentin Errera, Jean-Christopher Lambert, Piera Raspollini, Pasquale Sellitto, Mona Kosary, Beatriz Monge-Sanz, Enzo Papandrea, Bianca Maria Dinelli, Kaley Walker, Patrick Sheese, Umberto Rizza, Tiziano Maestri, Stefano Corradini, Lorenzo Cassini, Arun Jo Mathew, Manyatt Pramitha, Han-Li Liu, Nicholas Pedatella, Simone Tilmes

ESA Technical Officer	ESA budget heading
Alex Hoffmann **Division** Mission Science Division **Directorate** Directorate of Earth Observation Programmes	

DOCUMENT INFO

Reviewer

Reviewer	Organisation Short Name	E-Mail
All WP-Leader		

Document Control

Document version #	Date	Changes Made/Comments
0.1	12.11.25	First draft
1.0	20.12.25	Second draft
1.1	16.01.26	First complete version
1.2	22.01.26	Final version

Signature by issuing authority and/or lead author

Table of Content

1 Introduction

1.1 The CAIRT Mission

The Changing-Atmosphere Infrared Tomography Explorer (CAIRT) has been studied as a candidate for ESA's Earth Explorer 11 (EE11) satellite mission. After successful completion of Pre-Feasibility (Phase 0) studies, CAIRT has been selected in November 2023 as one of two mission concepts for Phase A studies. The scientific performance assessments, requirements consolidation and impact studies were performed as part of the Performance and Requirement Consolidation (PerReC) project. Results of the Phase A studies were summarized in the CAIRT Report for Mission Selection (RfMS) and presented at a User Consultation Meeting in July 2025 in Prague, Czech Republic. Based on these results, it was concluded that CAIRT has reached the required technical and scientific maturity to be implemented as EE11. In the competitive selection process, ESA's Advisory Committee for Earth Observation (ACEO) recommended the competing mission concept WIVERN to be implemented as EE11. ACEO conclusions are reported here: "CAIRT's scientific goals are both timely and important, addressing major unknowns with important societal benefits as well. While we recommended WIVERN as Earth Explorer 11, we also strongly encourage continued scientific studies and field campaigns for CAIRT to keep the door open for possible future implementation."

CAIRT's central mission objective is to provide the much-needed observations to resolve the connection between atmospheric composition, circulation, and climate change – from the troposphere to the edge of space.

Climate change is not restricted to the Earth's surface. In fact, the atmosphere is changing throughout its entire depth from the surface to the fringes of space due to anthropogenic emissions of greenhouse gases, pollutants, aerosols and their precursors, and the recovery from ozone-depleting substances (ODSs). This change is occurring against a naturally variable background influenced by, inter alia, volcanic eruptions and solar variability. The deep atmospheric region between the upper troposphere/lower stratosphere (UTLS) at about 5-10 km altitude and the lower thermosphere at about 100 km altitude is commonly called the middle atmosphere. The middle atmosphere is at the nexus of atmospheric climate system. The middle atmosphere connects distant regions, including coupling with the upper atmosphere and space environment, it provides predictability beyond typical weather time scales, and changes in its composition and aerosol load exert critical forcing of surface climate. The middle atmosphere is also the home of the ozone layer, that protects all life on Earth from harmful UltraViolet radiation. In addition to the effect of accelerated climate change, emerging challenges include the impact of wildfire smoke on the middle atmosphere, possible increased atmospheric impacts by rocket launches and satellite re-entry under upcoming satellite mega-constellations, and the possibility of deliberate aerosol injection into the stratosphere under solar radiation management or "geoengineering" attempts to counteract global warming.

The large-scale atmospheric circulation plays a central role in connecting the ongoing changes in the middle atmosphere (Figure 1). It is characterized by the tropics-to-pole Brewer-Dobson circulation in the stratosphere, and a summer pole to winter pole circulation in the mesosphere. The transfer of momentum by atmospheric waves plays a critical role in driving this circulation. Better understanding of the ongoing and predicted changes in the middle atmosphere requires new observations to diagnose the large-scale circulation, to quantify the wave-driving of the circulation and to investigate its impact on atmospheric structure and composition.

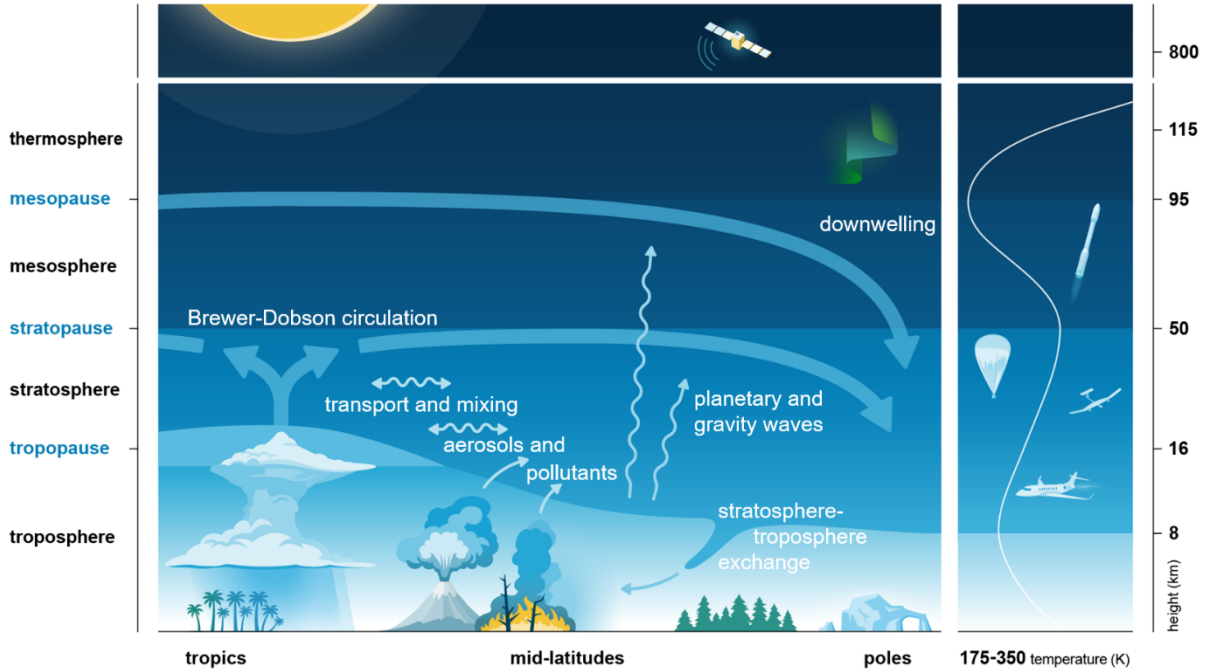

Figure 1: Schematic of the middle atmosphere wave-driven circulation and its intimate connection with atmospheric transport and composition.

CAIRT employs an innovative infrared limb imaging technology to observe processes and coupling simultaneously over the deep atmospheric region from the mid-troposphere at ~5 km altitude to the thermosphere at the edge of space at ~115 km altitude (Figure 2). Based on a concept of imaging Fourier-transform infrared spectroscopy and tomographic retrievals, CAIRT will provide, for the first time, global observations of atmospheric dynamics and composition in three dimensions (3D), well-resolved both vertically and horizontally. With this 3D capability, CAIRT will reveal atmospheric processes that have been largely unseen so far in a global way, such as the elusive gravity waves (GW) that play an important role in atmospheric dynamics, and remain an important source of uncertainties in current models. CAIRT will resolve atmospheric small-scale structures such as plumes of pollutants and aerosols injected into the stratosphere from wildfires and volcanic eruptions, or the pockets of reactive nitrogen oxides drawn from the thermosphere deep into the winter stratosphere. CAIRT will map sharp gradients of ozone and water across the tropopause that will help models produce more accurate weather forecasts.

There is an urgent and critical need for these observations, as emphasized by the World Meteorological Organization (WMO (GCOS-244), Action A2, 2022), and highlighted in several recent community perspectives, in particular warning against the “imminent data desert” and “observational gaps” in a large part of the global atmosphere (Añel et al., 2025; Mlynczak et al., 2021; Plane et al., 2023; Salawitch et al., 2025). The CAIRT mission will not only fill this critical gap, for which no other measurements will exist, but will do so with novel observations that will provide a step change in our understanding of the processes at play.

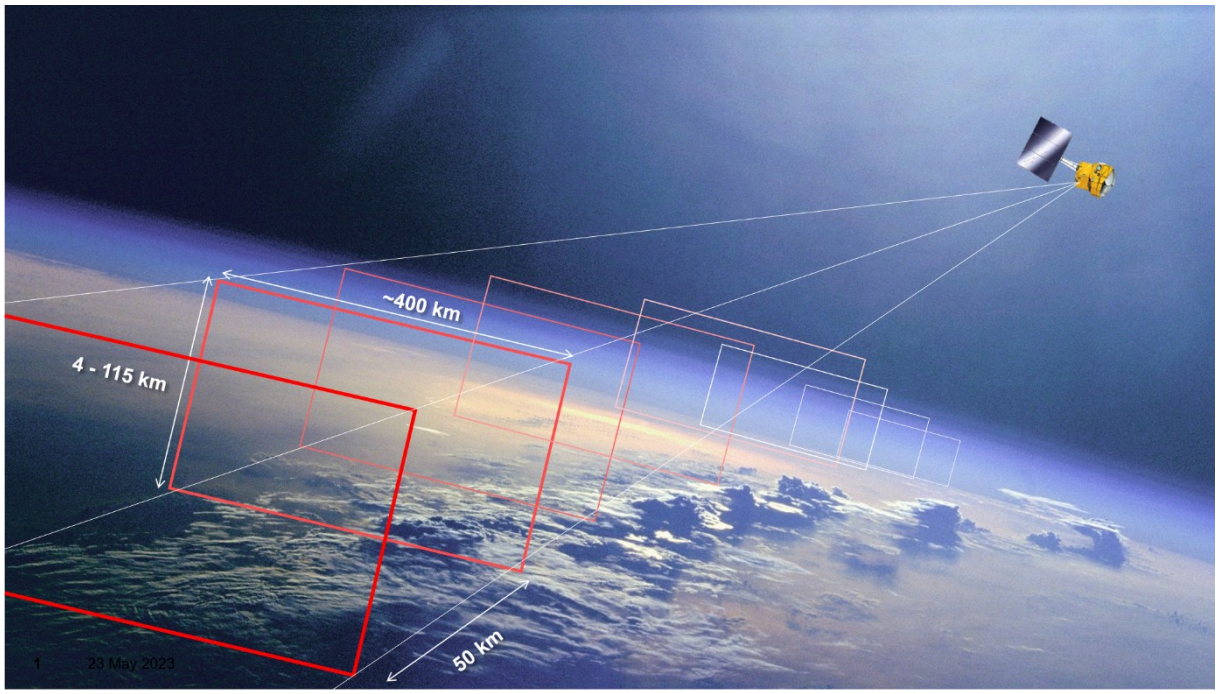

Figure 2: Illustration of the CAIRT observational concept. Every 50 km along track (corresponding to about every seven seconds) an infrared limb image with a tangent altitude of 4 to 115 km and with about 400 km across track is recorded. (Background image: NASA.)

Specifically, CAIRT's five science objectives are:

1. Diagnose the changing atmospheric circulation between the upper troposphere and the lower thermosphere, through observations of temperature, long-lived trace gases and derived age-of-air (AoA), from the global scale down to spatial scales associated with mixing and exchange processes.
2. Quantify the contribution of gravity waves (GWs) to the driving of the middle atmospheric circulation, identify their sources and investigate their propagation and dissipation, through observations of GWs between the lower stratosphere and the mesosphere, and at scales relevant for circulation change.
3. Investigate upper atmospheric coupling and concomitant regional surface climate variability associated with transient solar events and space weather through the downward flux of reactive nitrogen (NOy) from the thermosphere, and its impacts on stratospheric ozone.
4. Quantify lower atmospheric coupling associated with the lofting or injection of natural and anthropogenic plumes of pollutants and aerosol precursors into the upper troposphere and stratosphere, their impacts on composition, and their crucial role for climate forcing and feedbacks.
5. Resolve strong vertical gradients and fluxes of ozone and water vapour across the tropopause, facilitate the attribution of changes in middle atmospheric ozone, water vapour, and other constituents to changes in stratosphere-troposphere exchange, circulation, and chemistry, and improve our knowledge of the complex radiative-dynamic-chemical coupling governing our climate system.

1.2 The PerReC project

The CAIRT Phase A Mission Performance and Requirement Consolidation (PerReC) Activity was kicked off in June 2024. It was coordinated by Karlsruhe Institute of Technology (KIT, Germany) as prime contractor, with subcontracts with Forschungszentrum Jülich (FZJ, Germany), Instituto de Astrofísica de Andalucía (IAA-CSIC,

Spain), CNR (Italy), Royal Belgian Institute for Space Aeronomie (BIRA-IASB, Belgium), LISA-UPEC (France), and University of Oxford (UK). Following the Statement of Work, the activity was organised in ten tasks. Task 1 performed a self-evaluation of the Scientific Readiness Level (SRL); Task 2 provided a review of mission science and observation requirements; Task 3 provided Algorithm Theoretical Baseline Documents (ATBD), as well as product specification and validation planning documents; Task 4 encompassed the planning of the performance evaluation, including the provision of test data sets; Task 5 performed the scientific product performance evaluation; Task 6 was reserved for consultancy and support for end-to-end and system studies; Task 7 prepared the planning of case and impact studies; Task 8 provided an evaluation of scientific applications and the potential for societal impact; Task 9 included the consolidation of documentation, requirements, recommendations, and reporting; Task 10 encompassed scientific engagement, dissemination, mission promotion, and outreach.

The remainder of this executive summary of the PerReC activity is largely structured according to these ten project Tasks.

2 Task 1: Assessment of Scientific Readiness Level

The scientific maturity of the CAIRT mission concept was assessed by PerReC within ESA's EOP Science Readiness Level (SRL) framework. As a result of dedicated Phase A activities, SRL increased from SRL-4 to SRL-5. SRL-5 revolves mostly around mission performance assessment. The evidence for SRL-5 is provided along the following guiding questions:

1. ***Is a performance simulator in place and are the most important and significant processes and input parameters (including sources of uncertainty) properly represented?***

Yes. A CAIRT End-to-End Performance Simulator (CEEPS) was developed within a dedicated contract. Emphasis of CEEPS is on simulating the observing system, including orbit/attitude, viewing geometry, instrument physics and associated errors. CEEPS captures the entire data flow and processing chain from oversampled "true" radiance stimuli simulation over electronic signal generation and L1 processing to non-linear tomographic L2a retrievals. CEEPS is fully configurable to simulate different observing system configurations, errors, and auxiliary inputs. In addition, a Scientific Workbench (SWB), has been developed under the PerReC contract for rigorous, systematic, and fast performance evaluation.

2. ***Is an error propagation model in place allowing the rigorous computation of uncertainties (e.g. accounting for co-variant error effects) for measurement and observation data?***

Yes. CAIRT generally follows the World Climate Research Programme (WCRP)/Atmospheric Processes And their Role in Climate (APARC)'s Towards Unified Error Reporting (TUNER) community-defined approach towards unified error reporting, that set out to provide complete and consistent data characterisation in terms of uncertainty, resolution and content of a priori information for spaceborne temperature and composition sounders (von Clarmann et al., 2022, 2020). This methodology is conceptually aligned with the CEOS QA4EO framework.

3. ***Has a set of realistic and representative test scenarios and input scenes been established and are they scientifically justified?***

Yes. Various CAIRT test scenarios and input scenes have been established for different purposes. For systematic CAIRT total uncertainty and performance assessments the comprehensive and representative Extended Reference Scenarios database (ERS) (Errera, 2023) has been compiled. For scientific scenarios and impact assessments scenes based on high-resolution weather and climate models (the **European Centre for**

Medium-Range Weather Forecasts – Integrated Forecasting System (ECMWF-IFS), the Whole Atmosphere Community Climate Model with thermosphere and ionosphere eXtension (WACCM-X)) were compiled and used.

4. Is the simulator tested, verified / validated and applied for the predefined set of scenarios?

Yes. SWB and CEEPS have been applied to the predefined scenarios. A first intercomparison between SWB and CEEPS has been successfully performed. Compliance of all L2 product requirements has been verified through performance assessments.

5. Are all assumptions of the performance simulator documented and critically discussed?

Yes. All critical assumptions of the performance simulators (SWB and CEEPS) are documented in Algorithm Theoretical Baseline Documents (ATBD).

6. ***Has the robustness of the simulator been demonstrated against independent observations (e.g. campaign data)?***

Yes. The algorithms behind the performance simulators have been validated in a number of previous aircraft and balloon campaigns by intercomparison with independent observations. The CAREVALAB aircraft campaign in March 2025 demonstrated that data from a CAIRT-like viewing geometry can successfully be exploited in tomographic retrievals – as implemented in CEEPS.

7. Is a draft mission calibration and product validation strategy available & properly described?

Yes. A CAIRT Product Validation Strategy has been developed within the PerReC activity. Moreover, it should be noted that CAIRT retrievals are entirely based on physics-based radiative transfer theory and model, so that the mission does not rely on empirical calibration when inverting for L2a temperature and trace gas products.

8. Is there a demonstrated interest of users?

Yes. The urgent need for new limb observations has been addressed through a number of recent community papers, as well as by WMO-GCOS recommendations (GCOS-240, Action A30, 2021; GCOS-244, Action A2, 2022). A CAIRT user survey in 2024-2025 showed strong interest in CAIRT and its new data set from across ESA Member States and beyond.

9. Is there a first evaluation (of simulated or measured data) in applications?

Yes. A number of impact assessments were performed as part of the PerReC activity, including assimilation of simulated CAIRT products in Observing System Simulation Experiments (OSSEs). More details are provided in later sections of this report. CAIRT-dedicated peer-reviewed papers have been published in Phase A (Errera et al., 2025a; Rhode et al., 2024; Tirelli et al., 2025; Voet et al., 2025) and more are in preparation.

3 Task 2: Review of mission science and observation requirements

CAIRT Mission Objectives and observation requirements have been reviewed and consolidated as part of PerReC Task 2, documented in a technical note TN-1. To each of CAIRT's five Science Objectives there is a corresponding specific Mission Objective, that defines the geophysical target parameters to be observed. From these five Mission Objectives, specific observation requirements are derived (Table 1). These include the required vertical range, the required total uncertainty, and required vertical and horizontal resolution. It should be noted that total uncertainty and spatial resolution are not independent; in many cases a trade-off

between uncertainty and spatial resolution can be achieved. Review and consolidation of the observation requirements is based on: (a) existing user requirement documents such as WMO-GCOS or ESA-CCI; (b) performance of previous heritage instruments, such as MIPAS-ENVISAT or the Microwave Limb Sounder (MLS); (c) expected atmospheric variability, e.g. as represented by the Extended Reference Scenario climatology (ERS, as an example see **Figure 3**); (d) a scientific flow-down of observation requirements to achieve specific Mission Objectives, e.g. requirements to meet the <0.5 years for AoA in MO-P-1 or the GW parameters in MO-P-2.

Existing user requirement documents for ozone and water vapour in the middle atmosphere all agree that observations at higher horizontal and vertical resolution than available so far are needed (WMO-GCOS, ESA O3 CCI, ESA WV-CCI). Limb imaging tomography offers the unique possibility to achieve at the same time the required horizontal and vertical resolution of about 1-2 km vertically and 100-200 km horizontally. In many cases existing user requirements are very "aspirational" and go significantly beyond what has been possible with the existing observing system. A review of performance of relevant heritage instruments was therefore included in the consolidation of the CAIRT requirements. For many of CAIRT's L2 products no previous user requirements existed. For some, such as long-lived greenhouse gases in the ESA LOLIPOP CCI, requirements have been formulated for a somewhat different application, so are not directly applicable here.

Requirements for GW parameters have been derived in a scientific analysis and required uncertainty limits determined which allow for constraining the GW driving of the circulation and for identifying sources via ray-tracing.

3.1 Mission objectives and observation requirements

As a result of the review and consolidation the following primary Mission Objectives and observation requirements (Table 1) have been formulated.

MO-P-1: Observe atmospheric circulation throughout the lower stratosphere via AoA derived from long-lived tracers (e.g., SF_6, CFC-11, CFC-12, HCFC-22, N_2O) with a total uncertainty of $\lesssim$0.5 years ($\lesssim$0.25 years in monthly zonal means); and via suitable upper atmospheric tracers (CH_4, CO, temperature) up to the mesosphere and lower thermosphere (MLT).

MO-P-2: Determine the global distribution of GW momentum flux and drag and the associated phase speeds, by resolving amplitudes, wavelengths, and direction of GWs in a range of ~100 to ~2000 km horizontal and down to $\lesssim$3 km vertical wavelengths, from the lower stratosphere into the mid-mesosphere.

MO-P-3: Observe NO produced in the lower thermosphere and NOx (NO, NO_2) in the MLT during quiescent conditions and during geomagnetic storms, and quantify the total reactive nitrogen NOy (NOx, HNO_3, N_2O_5, $ClONO_2$) throughout the stratosphere.

MO-P-4: Quantify pollutants from biomass burning and anthropogenic origins (CO, PAN), sulfate aerosol and the atmospheric sulfur budget (H_2SO_4(l), SO_2, OCS) within the free troposphere and the lower stratosphere during enhanced conditions.

MO-P-5: Quantify the vertical and horizontal distribution of O3 and H2O throughout the middle atmosphere, and with particular emphasis on resolving strong gradients and spatial features within the UTLS.

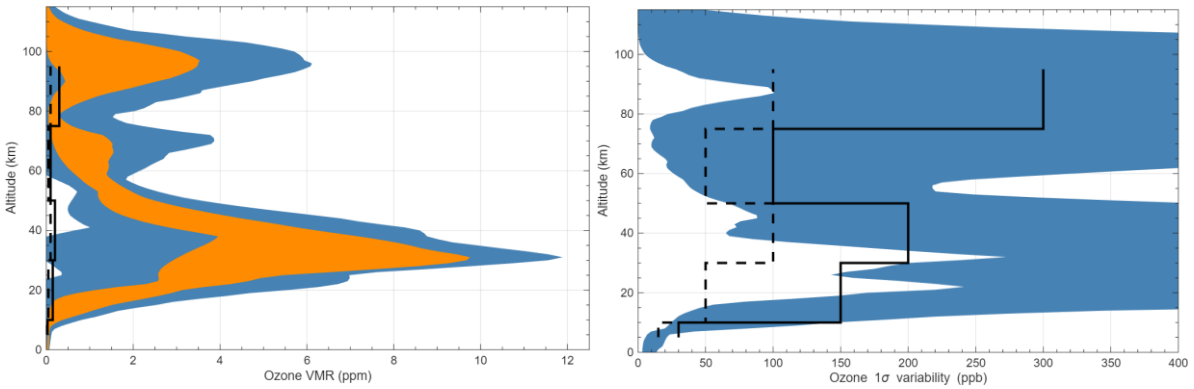

Figure 3: Ozone (O_3) distribution and variability computed from the Extended Reference Scenario (ERS) climatology. Left: Orange shading: Range of climatological mean O_3 profiles for different latitudes and seasons [MIN(MEAN),MAX(MEAN)]. Blue shading: Range of climatological O_3 profiles ±3 standard deviations [MIN(MEAN-3STD),MAX(MEAN+3STD)]. Right: O_3 variability from the ERS climatology. Blue shading: Range of variability (1 standard deviation) for different latitudes and seasons. Black solid lines: CAIRT threshold requirements, black dashed lines: CAIRT goal requirements.

Table 1. Overview of CAIRT observation requirements for the primary L2 products. MO: driving mission objective, FT: free troposphere, LS: lower stratosphere, US: upper stratosphere, LM: lower mesosphere, UM: upper mesosphere, LT: lower thermosphere. G: goal, T: threshold requirements.

Product	MO	Regions	Total uncertainty		Unit	Vert. res. (km)		Hor. res (km)	
			(G)	(T)		(G)	(T)	(G)	(T)
T	all	FT – LM UM LT	1 2 10	2 5 20	K	1 2 4	2 4 7	50 200 200	200 400 400
H_2O	5	FT LS US LM UM	5 5 5 500 500	10 10 10 800 800	% % % ppb ppb	1 1 2 2 3	2 3 3 4 5	100 100 100 200 200	200 200 300 400 400
O_3	5	FT LS US LM UM	15 50 100 50 100	30 150 200 100 300	ppb	1 1 2 2 2	2 2 3 4 5	100 100 100 200 200	200 200 200 300 400
CH_4	1	LS US LM	30	60	ppb	1 2 2	3 3 4	100 100 200	200 200 300
SF_6	1	LS	0.1	0.13	ppt	1	3	100	ZM
HCFC-22	1	LS	2	6	ppt	1	3	100	200
CFC-11	1	LS	10	25	ppt	1	3	100	200
CFC-12	1	LS	10	30	ppt	1	3	100	200
N_2O	1	LS US	10	16	ppb	1 2	3	100	200
CO	1, 4	FT LS US LM UM LT	20 20 40 100 700 2000	30 30 70 500 2000 5000	ppb	1 1 2 2 3 4	2 2 3 4 5 7	100 100 200 200 200 200	200 200 300 300 400 400
NO	3	LS US LM	0.2 0.2 2	0.5 1 20	ppb	1 2 2	4 4 4	100 200 200	300 300 300

		UM LT	100 5000	600 30000		3 3	5 5	200 200	400 400
NO_2	3	LS US LM	0.2 0.2 2	0.5 0.5 5	ppb	1 2 2	3 3 4	100 200 200	300
HNO_3	3	LS US LM	0.2 0.2 0.5	0.5 0.5 2	ppb	1 2 2	3 3 4	100 200 200	300 300 400
N_2O_5	3	LS US	0.2	0.5	ppb	1 2	3	100 200	300
$ClONO_2$	3	LS US	0.1 0.2	0.25 0.5	ppb	1 2	3	100 200	300
PAN	4	FT – LS	0.04	0.1	ppb	1	2	100	200
OCS	4	LS	0.05	0.15	ppb	1	2	100	200
SO_2	4	LS	0.1	1	ppb	1	2	100	200
H_2SO_4 (l)	4	LS	0.1	0.3	$\mu m^3/cm^3$	1	2	100	200

3.2 Applications and Societal Impact

3.2.1 Middle-atmosphere monitoring

There is an urgent need for continued monitoring of middle atmosphere dynamics, structure and composition:

- The recovery of the ozone layer in the Northern Hemisphere has stalled, in contrast to expectations and possibly due to changes in the middle atmosphere circulation.
- Smoke from recent large wildfires has been observed to enter the stratosphere, leading to an increase in stratospheric aerosols exceeding the effect of small to medium-size volcanic eruptions, forcing surface climate through their interaction with solar radiation and destroying stratospheric ozone. With climate change, the impact of wildfires is projected to increase further.
- There are growing concerns that the increase of space-debris from upcoming satellite mega-constellations, together with emissions from increasing numbers of rocket launches, will affect the middle atmosphere composition in yet unknown ways.
- The contentious but conceivable injection of stratospheric aerosols to counteract global warming (geoengineering) requires a better understanding of potential adverse effects before any implementation, and close monitoring during any subsequent attempts.

While the future observing capacity for ozone is reasonably assured (Salawitch et al., 2025), there is in particular a notable lack of future observations of tracers to diagnose changes in atmospheric transport and to attribute observed changes in composition. The 2022 WMO/UNEP Scientific Assessment of Ozone Depletion ((WMO et al., 2023)- GAW-278), 2023, p. 163) quotes the need to *"continue limb emission and infrared solar occultation observations from space" that are "necessary for global vertical profiles of many ozone- and climate-related trace gases"* as one of the *"key systematic observations recommendations*". CAIRT's observation requirements of ozone, water vapour, long-lived tracers to diagnose changes in atmospheric transport and AoA, ozone depleting substances (e.g. CFCs, but also N_2O), key halogen and nitrogen compounds are in line with these societal needs. The hyperspectral observations with a wide spectral bandwidth and relatively high spectral resolution provide an opportunity for the detection and retrieval of relevant additional gases and aerosols to respond to upcoming challenges, beyond CAIRT's primary L2 products. E.g., a first feasibility study as part of the PerReC activity has shown the possibility with CAIRT to detect spectral signatures of aluminium oxide Al_2O_3 in the mesosphere from satellite re-entry under a future mega-constellation scenario.

3.2.2 Improving retrievals of tropospheric gases

Height resolved limb observations can together with nadir observations provide important constraints for the retrievals of tropospheric gases. This is in particular important for the retrieval of tropospheric ozone, otherwise very challenging, as only about 10% of the total ozone column are located in the troposphere and about 90% in the stratosphere. Reducing the uncertainty in the stratospheric ozone contribution therefore has a strong impact on improving tropospheric ozone retrievals. Also, for other compounds, such as methane, better constraining the stratospheric contribution can help to improve the retrieval of the tropospheric distribution, including the quantification of emission sources.

3.2.3 Assimilation of CAIRT data for numerical weather prediction and climate reanalyses

Improving the representation of water vapour and ozone in the UTLS in numerical weather forecasting models has been shown to lead to significant improvements in meteorological predictions (e.g. Hogan et al., 2017; Monge-Sanz et al., 2022). Assimilation of water vapour data from Aura/MLS in ECMWF's forecasting system (Semane and Bonavita, 2025) improves long-standing temperature biases in the model through improved water vapour interaction with radiation, as well as sharpening and strengthening the tropopause. With the imminent end of the MLS mission, there is a strong need for continued vertically resolved water vapour profiles in the UTLS region. Impact studies performed within CAIRT Phase A have shown that the assimilation of CAIRT water vapour observations is quantitatively comparable to MLS in constraining water vapour in the UTLS region.

Most weather forecasting centres have raised their model top altitude well into the upper stratosphere or even into the mesosphere to improve forecast skill (Scaife et al., 2022). However, few observations exist above the lower stratosphere to constrain models there. CAIRT will rectify this situation. There is currently a revolution going on in the use of Artificial Intelligence (AI) models for weather and climate prediction. Particularly exciting is recent progress in AI-based weather forecasts trained and initialized directly from satellite observations (Allen et al., 2025; McNally et al., 2024) or as part of online hybrid models (Farchi et al., 2024). As discussed by McNally et al. (2024), this approach, trained and based on raw (Level-1) satellite data, offers the potential to exploit the full observational information content (e.g., in clear sky and cloudy conditions) and can be directly extended to other Earth System domains, including atmospheric composition. These new data-driven applications are not only computationally/cost effective but can leverage observational data so far not (or not fully) exploited. CAIRT, with its unmatched data density – some 80,000 profiles per day, covering essentially the whole atmosphere and highly complementary to any other existing or planned satellite data products – can play a transformative role in future atmospheric data-driven model development and applications.

3.2.4 Validation of atmospheric models

Validation of models and guidance of further model development is an important application of CAIRT observations. For chemistry climate models, the SPARC CCM-Val activities, that has evolved into APARC's Chemistry Climate Modelling Initiative (CCMI), have paved the way for a process-oriented validation of models. The SPARC CCMVal-2 Report (SPARC Report No. 5, 2010) has already stated clear requirements and recommendations for future vertically resolved observations in the stratosphere and upper troposphere: "Long-term vertically resolved data sets of constituent observations in the stratosphere are required to assess model behaviour and test model predictions. This includes ozone, but also other species that can be used to diagnose transport and chemistry. The current set of GCOS Essential Climate Variables is not sufficient for process-oriented validation of CCMs. More global vertically resolved observations are required,

particularly in the UTLS. As CCMs evolve towards including tropospheric chemistry, lack of observations in this region will become a major limitation on model validation." Since the time of writing in 2010, the availability of vertically resolved data in the stratosphere and upper troposphere has not improved and these requirements are still valid. CAIRT's observational requirements and the assessed performance are aligned with these requirements and the expected impact of CAIRT data for model validation is well established.

3.2.5 Volcanic ash detection

Volcanic eruptions emit large amounts of gases and particles into the atmosphere (Fromm et al., 2014), causing severe impacts on atmosphere (Robock, 2000), climate (Robock, 2013), life on Earth (Forbes et al., 2003), human society (Robock, 2010; Zehner, 2010) and aviation (Prata and Tupper, 2009). An impact study has been conducted as part of the PerReC activities to show the capabilities of CAIRT to improve detection and characterization of volcanic ash clouds in the context of aviation safety (see Section 6.6 below).

4 Task 3: Algorithm Theoretical Baseline Documents

Once the CAIRT science and mission requirements are defined as described in the previous section, this task has the objective to study how the scientific needs can be translated into Earth Observation (EO) data products and how these products are generated from the observations. The first useful product in the processing chain are the Level 1b (L1b) spectra, which are calibrated and geolocated emission spectra; these have to be generated in Near Real Time (NRT) since they are directly suitable for data assimilation into Numerical Weather Prediction (NWP) and atmospheric composition models. Next, these spectra are used by the Level 2a (L2a) processor to retrieve temperature and all trace species. These are then used to generate Level 2b (L2b) products. **Figure 4** provides a high-level overview of the L2 processing chain, which produces the various L2a and L2b data products. Details on the content and characterization of L1b, L2a, and L2b products are given in DEL-05.

CAIRT observes the atmosphere over a wide range of elevation and azimuth angles, and – due to the high sampling rate - with multiple overlapping lines-of-sights. This enables true 3D tomography: the L2 processor can reconstruct the atmospheric state at unprecedented spatial resolution. The used scientific data processing scheme and algorithms are grounded in well-established methods applied to solving inverse problems for atmospheric sounding. Due to the increased problem sized, they have to be adapted to dealing with large-scale 2-D and even 3-D tomographic retrievals. Different approaches are possible to keep the retrieval manageable, either by sequentially following along the orbit or using larger blocks of slightly overlapping consecutive acquisitions. The JURASSIC2 algorithm, used for the analysis of both simulated CAIRT data and real CAIRT prototype GLORIA balloon/aircraft measurements, is capable of both 2-D and 3-D inversions.

The KOPRA forward model, including non-LTE capability and the possibility of computing 2D Jacobian, is used for the analysis of performances and it is also part of the SWB described in Section 5.1.

Starting from the L2a products, CAIRT will also deliver L2b products tailored to key mission objectives: gravity-wave parameters derived by high resolution temperature observations, mean age of air, derived by long-lived species, and total reactive nitrogen (NOy), derived by reactive nitrogen species.

The L2b GW products consist of wave vector, amplitude, and phase for individual events, along with derived quantities such as intrinsic phase speed, momentum flux, and GW drag.

Since large-scale planetary waves may dominate the temperature observations, before the GW estimation the global-scale background has to be removed. To this purpose, the Python toolbox GLOFI was developed

to remove large-scale structures and extract small-scale GW perturbations. Tests with simulated CAIRT/ERA5 data show that GLOFI accurately isolates GW signals and reproduces reference perturbations. After this, the S3D finite-volume sinusoidal fit method was adopted for CAIRT analysis, which determines a few dominant waves per atmospheric volume and which has been validated in numerous recent studies (Rhode et al., 2024).

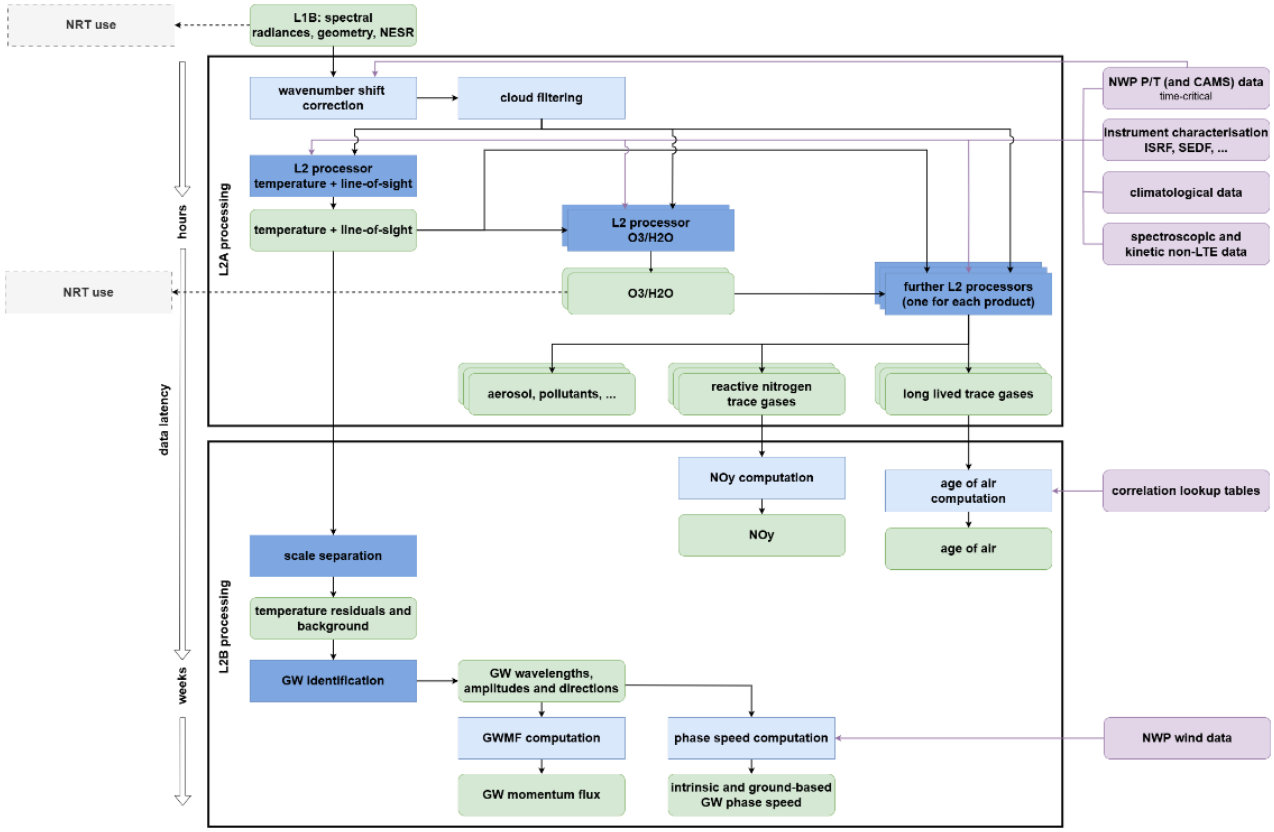

Figure 4: CAIRT L2 processing scheme and data production tree, depicted with an indicative time dimension (product latency increasing from top to bottom). Products in green, auxiliary data inputs in purple, processors and lighter processing steps in dark and light blue, respectively. Processing to higher-level data products and joint processing with data from MetOp-SG are not reported in this scheme.

Concerning the estimation of the mean-age of air, a new multi-species method has also been completed. By exploiting compact correlations among six satellite-measurable trace gases (CFC-11, CFC-12, HCFC-22, CH_4, N_2O, SF_6), the method achieves mean-age uncertainties below 0.3 years up to ~25 km and captures small-scale seasonal patterns (Voet et al., 2025). Comparisons with GLORIA-B observations confirm its reliability and indicate that ERA5 underestimates circulation strength.

The NOy L2b product is computed as the sum of the major reactive nitrogen species retrieved in L2a: NOy = NO + NO_2 + HNO_3 + $ClONO_2$ + 2×N_2O_5. It is provided on the same grid as the L2a products, with characterisation quantities derived from the ones of the L2a products.

CAIRT will fly in loose formation with MetOp-SG-A, enabling complementary atmospheric measurements with nadir instruments like IASI-NG. Two main strategies exist for data combination: synergistic retrieval, which integrates all measurements into a single complex system, and a posteriori combination, which merges previously retrieved products more efficiently. The approach followed to investigate possible advantages of the synergy strategy is the Complete Data Fusion (CDF) method (Ceccherini et al., 2015) extended to handle tomographic products (Tirelli et al., 2025). CDF is an a posteriori approach that combines independent remote sensing data into a single estimate. CDF accounts for retrieval errors, correlations, and sensitivity,

offering results equivalent to synergistic retrieval when the linear approximation of the forward models is appropriate in the range of the individual retrieval results.

Finally, CAIRT's ambitious objectives and novel measurement capabilities require a comprehensive validation strategy. The Product Validation Plan (PVP, DEL-06) describes how all Level-2 and higher-level data products (e.g., stratospheric age of air, reactive nitrogen, GW parameters) will be independently validated, detailing required standards (frameworks, protocols, methods and metrics), Fiducial Reference Measurements (FRM, Goryl et al., 2023) and other validation data, supporting models, campaigns, and tools to assess data quality, validate uncertainty characterization (e.g., Sofieva et al., 2019; Verhoelst et al., 2025), and evaluate compliance with mission requirements. Current best practices and community developed strategies are used to provide context and their application to CAIRT data product validation is also discussed in the PVP.

5 Tasks 4 and 5: Performance assessment

5.1 Scientific Workbench

The Scientific Workbench (SWB) was developed for measurement requirement consolidation and performance analysis as well as to support impact studies. It is a suite of tools for: (1) constructing comprehensive L2a uncertainty budgets with full L1→L2 error propagation, (2) evaluating L2b product performance, and (3) generating large emulated L2a datasets for science impact studies. **Figure 5** schematically overviews the SWB. Detailed algorithms have been described in ATBDs.

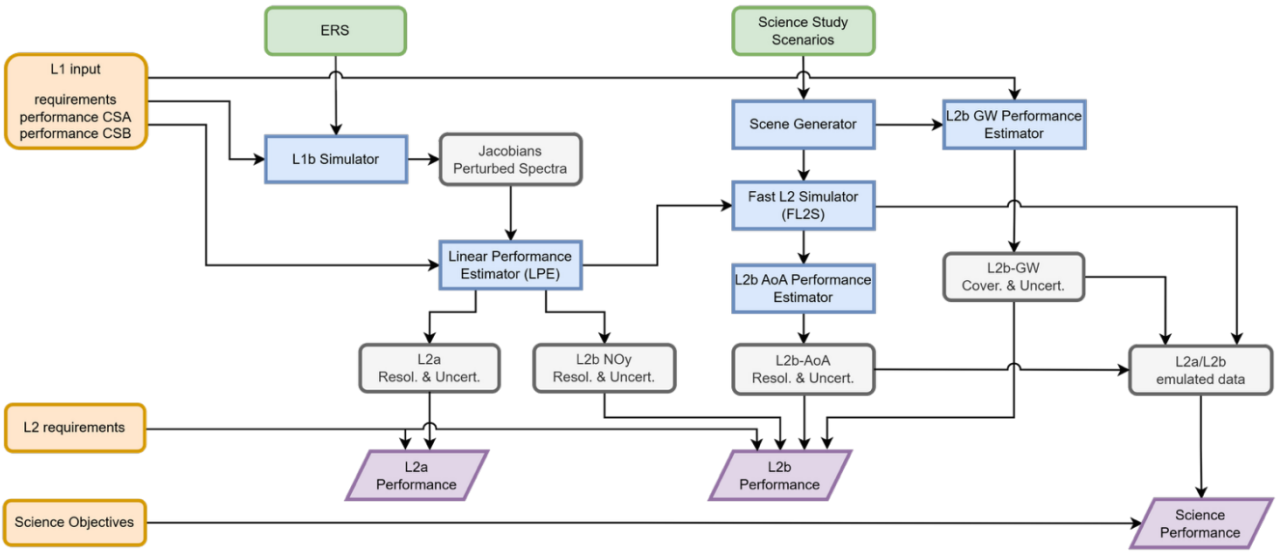

Figure 5: Schematic overview of the SWB, showing its modular architecture with individual components highlighted in blue boxes.

The L1b Simulator (instrument model) parameterizes the CAIRT payload and uncertainties for performance analyses. Driven by measurement requirements and instrumental parameters, it uses a database of vertically oversampled atmospheric pencil-beam (i.e. with infinitesimal System Energy Distribution Function (SEDF)) radiance- and Jacobian spectra across ERS climatology conditions, including difference spectra simulating instrumental/atmospheric/spectroscopic perturbations. The radiative transfer and non-LTE computations for this database are performed with KOPRA and GRANADA, respectively. Pencil-beam spectra/Jacobians are convolved spatially with the SEDF and spectrally with the Instrument Spectral Response Function (ISRF) according to instrument specifications on vertical and spectral sampling, resolution and coverage.

The Linear Performance Estimator (LPE) ingests Jacobians and perturbation spectra from the L1b Simulator to apply linear retrieval theory (Rodgers, 2000), extended to tomographic 2D retrievals. It computes 2D averaging kernels and L2a uncertainties via Gaussian error propagation (taking into account error covariances) or Monte Carlo (MC) ensembles. It propagates L1 and atmospheric uncertainties through temperature and LOS to subsequent trace gas retrievals, following MIPAS error reporting (von Clarmann et al., 2022). Temporally uncorrelated uncertainties beyond noise (e.g., elevation pointing jitter) are handled by 1D retrieval simulations.

The Scene Generator produces realistic geophysical scenes for L2a/L2b evaluation and impact studies, capturing dynamical/chemical variability including aerosols and clouds.

The Fast Level-2 Simulator (FL2S) emulates CAIRT L2a data for performance show-cases and impact assessments by interpolating LPE-derived 2D averaging kernels and error terms (from the ERS climatology) to scene grids and, applying convolution, yielding a computationally efficient parametric retrieval response. Calibration errors are sampled from Monte-Carlo (MC) perturbation ensembles; measurement noise is generated via covariance decomposition to preserve spatial correlations. The FL2S demonstrates performance on realistic inputs, provides inputs for L2b estimation, and generates validation datasets against CEEPS.

L2b algorithms and error models support products such as mean AoA and GW parameters. L2b NO_y performance is directly derived from LPE results of the single constituent species.

The L2b AoA Performance Estimator quantifies AoA uncertainties and spatial resolution following Voet et al. (2025), using tracer–tracer correlations among SF_6, CFC-11, CFC-12, HCFC-22, CH_4, and N_2O. It leverages the Chemical Lagrangian Model of the Stratosphere (CLaMS) simulations (ERA5-driven) providing these tracers plus an ideal clock tracer. L2a data with realistic uncertainties are simulated via FL2S; inferred AoA and uncertainties are compared to the ideal clock via zonal mean differences.

The L2b GW Performance Estimator addresses the non-linear nature of GW derivation using MC with non-linear tomographic temperature retrievals (JURASSIC). Performance is evaluated via zonal mean differences between L2b results from MC members and S3D analyses of “true” model temperature perturbations. Because background removal provides results largely insensitive to spatially/temporally correlated errors, MC perturbations are limited to measurement noise: pencil-beam spectra are perturbed with white noise, 16 MC instances are retrieved tomographically, followed by S3D analysis. For each event, mean and standard deviation of GW parameters (horizontal/vertical wavelength, amplitude, direction) are computed and aggregated (e.g., zonal means). A schematic overview of the GW L2b performance estimation is provided in Figure 6.

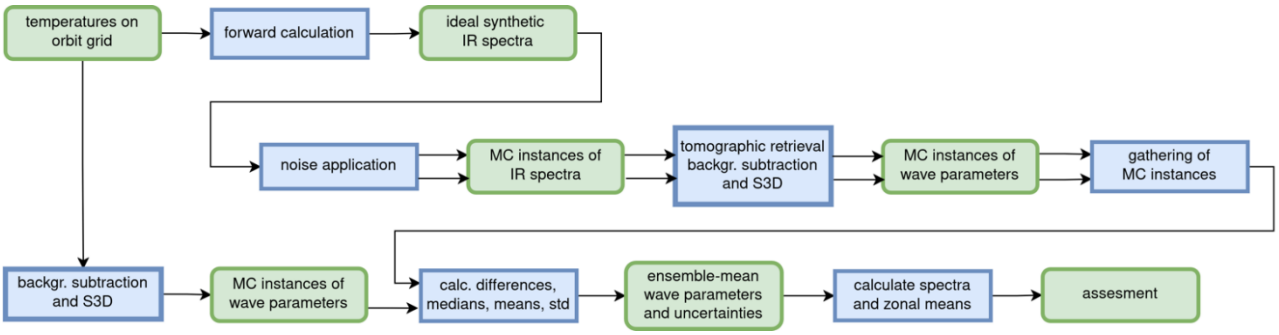

Figure 6: Schematic overview of the L2b GW performance estimation using MC analyses.

5.2 Measurement requirements consolidation

CAIRT measurement requirements were iteratively refined to satisfy L2a requirements. For all L2a products, the combined uncertainty and spatial (horizontal and vertical) resolutions arising from L1b measurements must comply with L2a specifications.

Given the many uncertainty sources and diverse L2a products, an optimized characterization approach was implemented. Using the LPE, instrument specifications and L1b uncertainties are mapped to L2a total uncertainty and spatial resolution for all primary CAIRT geophysical products. The metric for combined spatial resolution is the spatial volume-resolution ('hxvres'), defined as the volume around a retrieval grid point containing one degree of freedom (one independent piece of information). 'hxvres' is compared to volumes derived from resolution specifications to assess compliance. For the optimisation, analogous metrics for horizontal and vertical resolution are evaluated separately to enable trade-offs via tuning of the retrieval regularization.

Using these definitions, a metric to summarize the overall performance is defined as follows: at each altitude level for every ERS atmosphere, the estimated spatial resolution and total uncertainties are normalized by the corresponding goal and threshold requirement values. The resulting ratios are then averaged across all ERS atmospheres and altitude levels within the altitude regions defined for the L2a requirements. These mean ratios were subsequently classified into four categories for L2a requirement verification (**Table 2**).

Table 2 L2a requirement categories applied to L2 performance metrics (G: goal; T: threshold requirement).

Cat.	Performance evaluation	Assessment (example: predicted [p] vs required [G/T] uncertainty *u*)
1	Exceeds (better than) goal	$u_p/u_G \leq 1$
2	Between goal and threshold	$u_p/u_G > 1$ and $u_p/u_T \leq 0.8$
3	Threshold compliant	$0.8 > u_p/u_T \leq 1.2$
4	Non-compliant	$u_p/u_T > 1.2$

Many L1b instrument-model effects represent calibration and characterization knowledge requirements. Observing system performance (e.g., Noise Equivalent Spectral Radiance (NESR), pointing jitter) further impacts measurements.

External auxiliary inputs to retrievals - such as atmospheric priors, non-LTE parameters above the stratosphere (López-Puertas and Funke, 2015), CO_2 concentrations, and spectroscopy - also affect outputs. External-data uncertainties arise from imperfect knowledge of non-retrieved atmospheric parameters that affect observed radiances. In particular, CO_2 uncertainties primarily impact temperature retrievals in the mesosphere-lower thermosphere (MLT) and propagate to subsequent trace-gas inversions. Errors from emissions of other trace gases are largely mitigated by appropriate spectral-window selection or by jointly fitting these species with the target L2 parameter; hence, they are excluded from the LPE-based assessment. Additional parameters, like atomic O and N (N^4S, N^2D), are required to model non-LTE populations of CO_2, O_3, H_2O, NO_2, NO, and CO. Their uncertainties, together with those of NLTE-specific auxiliary data (e.g., collisional rate coefficients, photolysis rates; NLTE kinetics), are incorporated based on a comprehensive MIPAS data-analysis review. While no formal requirements are set for these auxiliary data, their uncertainties are accounted for in performance assessments.

Figure 7 summarizes the uncertainty propagation used in the L2 requirement consolidation as well as in the performance assessment. Observing-system effects are represented by instrument-specific L1b characteristics (spectral, radiometric, geometric, and calibration knowledge) defined during measurement requirement consolidation.

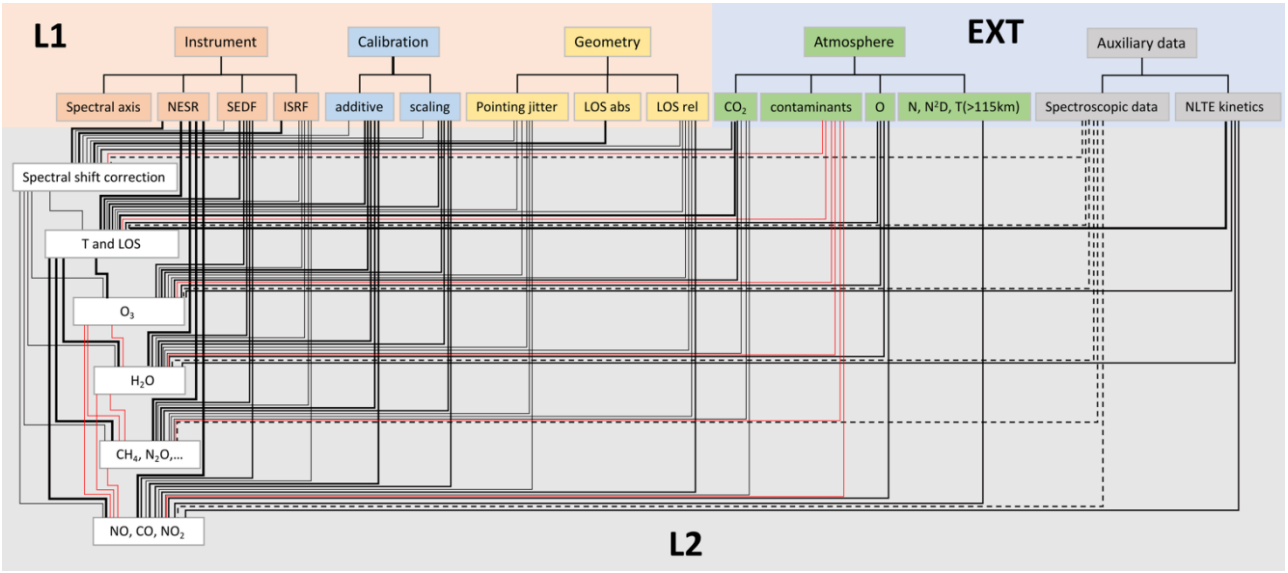

Figure 7: Uncertainty propagation from L1 products and external data (EXT) to L2. Pathways shown in red are analyzed exclusively with CEEPS; all others are treated by the SWB's LPE. Spectroscopic data uncertainties are assessed but excluded from the total uncertainty budgets. Line thickness qualitatively indicates the relative contribution of each source.

In **Figure 8** a top-down breakdown of L2a performance into key L1b requirements (radiometric, spectral, and geometric) is provided and can be read bottom-up to show how observing system and L1b data properties map to geophysical performance. Fulfilling the L1b requirements is not sufficient to meet L2a targets; additional optimization in L1 or L2 processing reduces uncertainties, notably in spectral (wavenumber) calibration, elevation pointing, and mitigation of off-axis signal contributions by diffraction and scattering for limb sounding with large vertical FoV and large dynamic range of spectral radiances (SEDF knowledge).

Figure 9 summarizes relative contributions of individual measurement requirements to threshold L2a total uncertainty by parameter and atmospheric region, computed as mean values across ERS atmospheres and specified altitude ranges. These numbers are derived for the threshold measurement requirements as in the Mission Requirement Document MRD (ESA Earth and Mission Science Division, 2025). The top three contributors per case are highlighted. NESR is the dominant driver of L2a uncertainty in most conditions; it is the only contribution routinely propagated within optimal-estimation retrievals, whereas the more systematic uncertainties are assessed offline. Independent contributors are combined as 'Root Sum of Squares'. An aggregate estimate of external error sources is shown for comparison; spectroscopic errors are excluded here and will be treated separately in future work. The rightmost columns demonstrate that threshold-level measurement requirements satisfy L2a targets for total uncertainty as well as spatial resolution.

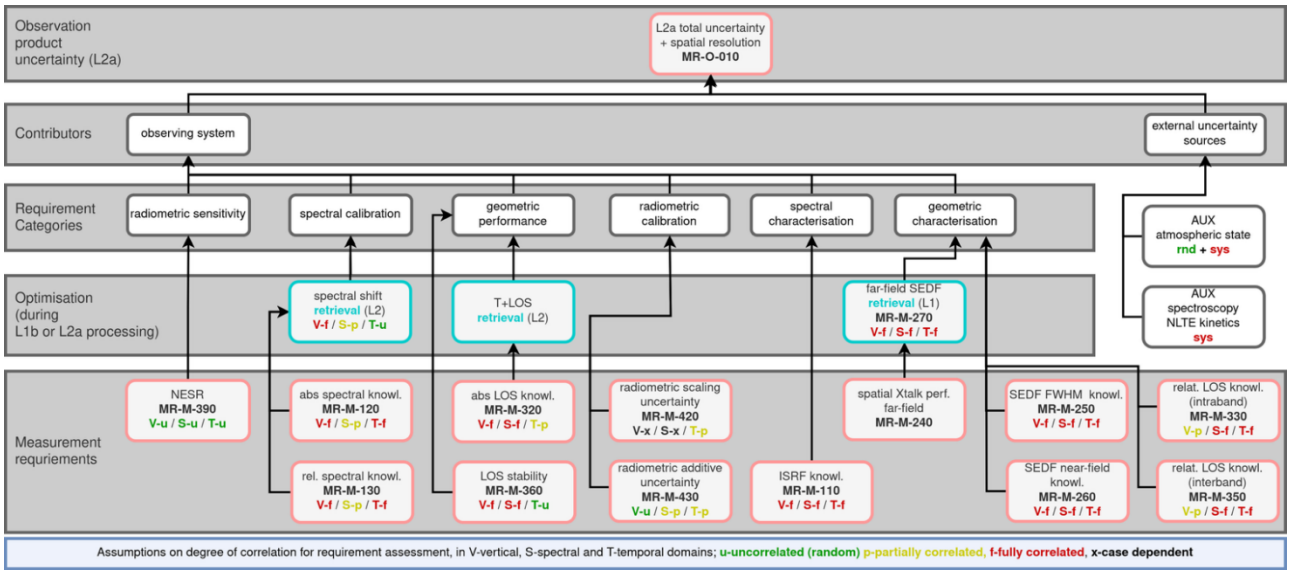

Figure 8: Breakdown of L2a performance requirements (uncertainty, spatial resolution) into contributing terms and measurement requirements, including a retrieval-stage optimization layer; external uncertainties shown but excluded from the flow-down.

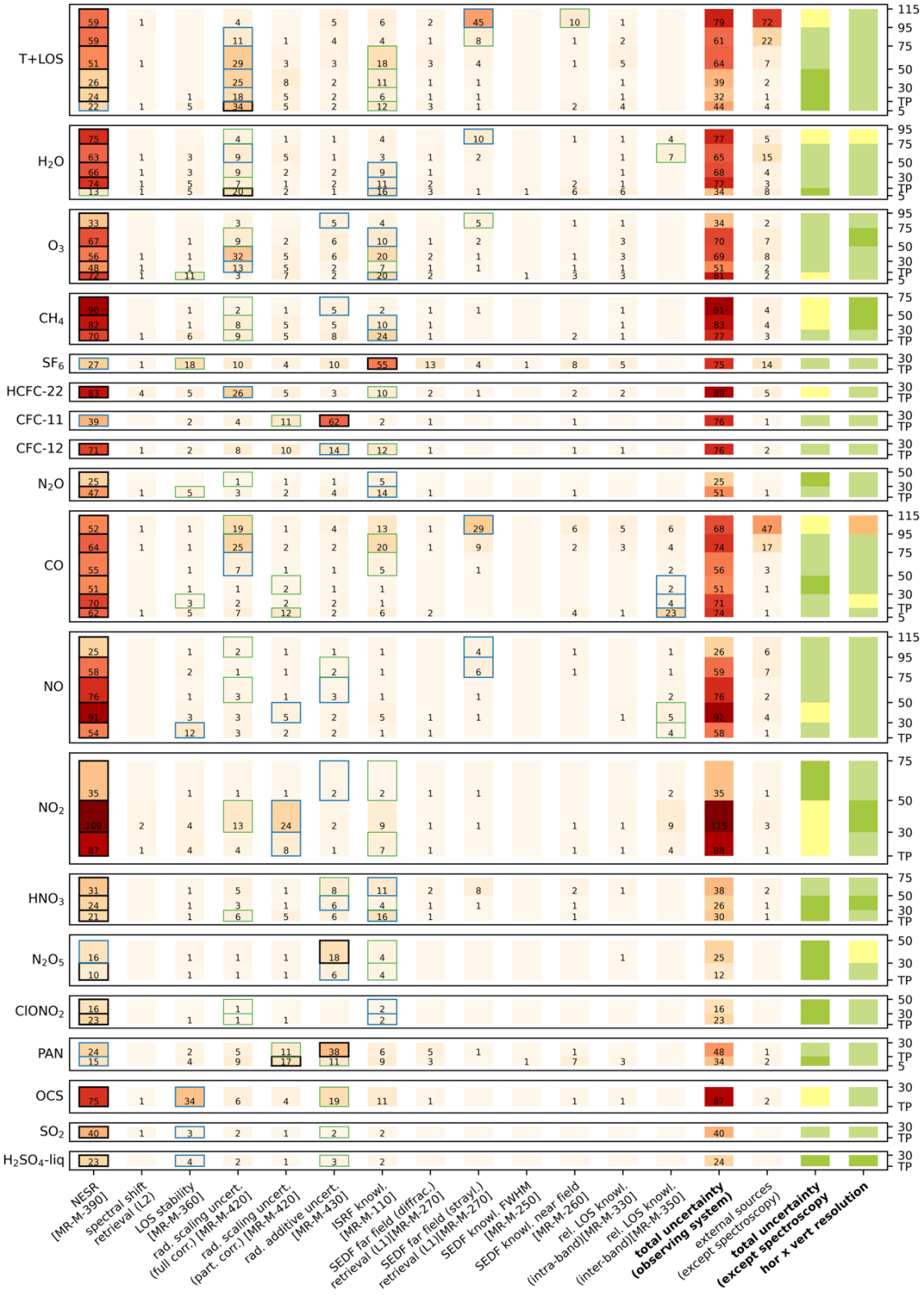

Figure 9: Contributions (in %) of measurement requirements (all at their threshold values and breakthrough for Middle Wave InfraRed -band NESR) to the specified threshold L2a total uncertainty requirements. For each L2a parameter in each vertical/altitude bin (y-axis on the right), the three dominant contributors to uncertainty are in boxes (black/blue/green, in order of their impact). Two rightmost columns: total uncertainty (including external sources except spectroscopy) and spatial resolution (hxvres) compared to L2a requirements, averaged over ERS climatology and vertical bins (see Table 2 for color scale).

5.3 Mission performance evaluation

System performance is propagated to the L2a and L2b products using the performance-simulation tools provided by the previously described SWB framework. Additionally, for application to realistic atmospheric scenes, a variety of geophysical test datasets (TDS-G) have been established. An overview of these datasets used in the CAIRT performance evaluation is provided in **Table 3**.

Table 3 Geophysical Test Datasets (TDS-G) used in the CAIRT performance evaluation.

TDS-G	Scenario	Source	SWB
1	Homogeneous	ERS climatology: April mid-latitude daytime used in CEEPS	Requirement consolidation; L2a performance evaluation
3a	GW A	WACCM-X high-resolution run: nudged to ERA-5 snapshot on 21 Jan 2019	L2b performance evaluation (GW): based on JURASSIC full tomographic retrievals
3b	GW B	ECMWF analysis: snapshot on 21 Jan 2019	Same as TDS-G-3a
4	Whole atmosphere	WACCM-X high-resolution run: nudged to MERRA-2 snapshot on 18 Feb 2019 1.5h data at 5-min time res.	LPE/FL2S validation with CEEPS results
5	AoA	CLaMS model run: snapshot on 6 Feb 2011	L2b performance evaluation (AoA): based on L2a LPE results

Results of the L2a performance estimations for the threshold measurement requirements have already been illustrated above (**Figure 9**). Here the L2a performance on basis of expected L1b characteristics of Concepts A and B is assessed. The focus is on the predicted NESR as the dominant contributor to total uncertainty. Additional system specifications (SEDF and vertical/horizontal sampling) are included as needed in the instrument model. All other L1b performances and uncertainties (beyond NESR, SEDF, and sampling) are assumed at requirement threshold values.

Figure 10 - **Figure 13** present examples of estimated performance figures for temperature and ozone for the two industry concepts, respectively, using the resolution and uncertainty metrics. Alongside total uncertainty, individual components are shown: (i) random uncertainties from spatially/temporally uncorrelated errors, (ii) calibration uncertainties that act systematically over short intervals tied to calibration periods but average as random at longer scales; and (iii) systematic uncertainties from spatially/temporally correlated errors that bias L2a products.

Additionally, FL2S simulations were run for whole-atmosphere scenes (TDS-G-04 in **Table 3**), using LPE outputs. Synthetic CAIRT L2a data from both concepts are compared with the model truth in the right panels of **Figure 10** - **Figure 13**. The comparison shows that CAIRT reproduces wave-induced small-scale temperature features and filamentary ozone structures with high fidelity, even under strongly perturbed NH polar-winter conditions characterized by an elevated stratopause over the North Pole (≈30 km above mid-latitudes) and record-low temperatures below. Differences exceeding the estimated absolute uncertainty can occur due to "smoothing" errors, since averaging kernels were not applied to the model truth.

The comprehensive assessment for both concepts as well as for the threshold requirements is summarized in **Figure 14** to **Figure 16** for all primary L2a targets and the L2b product NO_y. Relative to the observational requirements, L2a results meet all primary geophysical data specifications, with the exception of night-time CO in the MLT, which is not considered mission-critical.

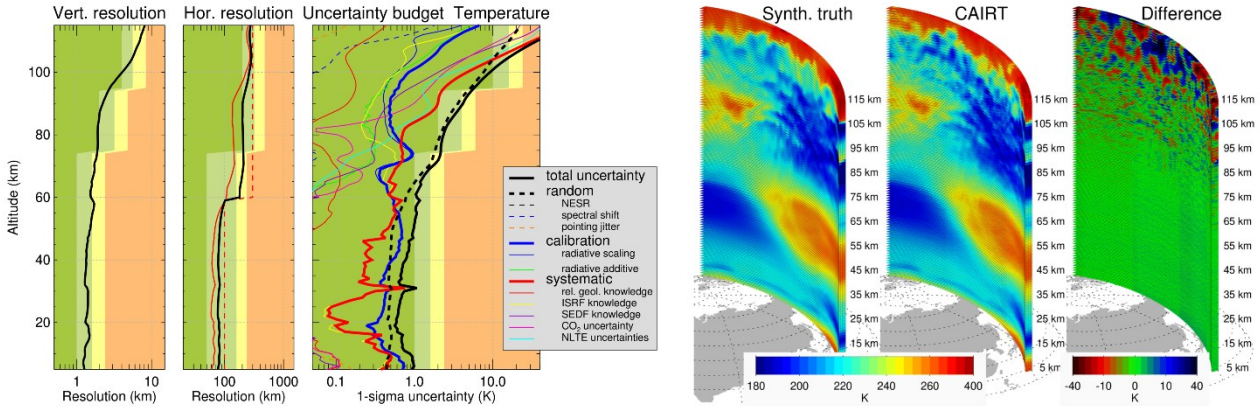

Figure 10: Left part: L2a performance estimation for temperature for Concept A considering all ERS atmospheres. Background shading corresponds to the L2a requirements (Table 2). The total error is the 1σ equivalent width of an error distribution, calculated as the geometric sum of all random and systematic components assessed. Vertical resolution is Δzi/(Σj'Aij,ij'). In the horizontal resolution sub-plot, red solid lines are along-track resolution (Δy (Σj' Aij,ij')/Aij,ij)), dashed red lines across-track binning. The black line corresponds to the area-related horizontal resolution hres=sqrt(altres × act) for which the requirements are defined. Right part: "true" temperature and emulated CAIRT data, as well as their differences, for an orbit segment across the TDS-G-04 scenario.

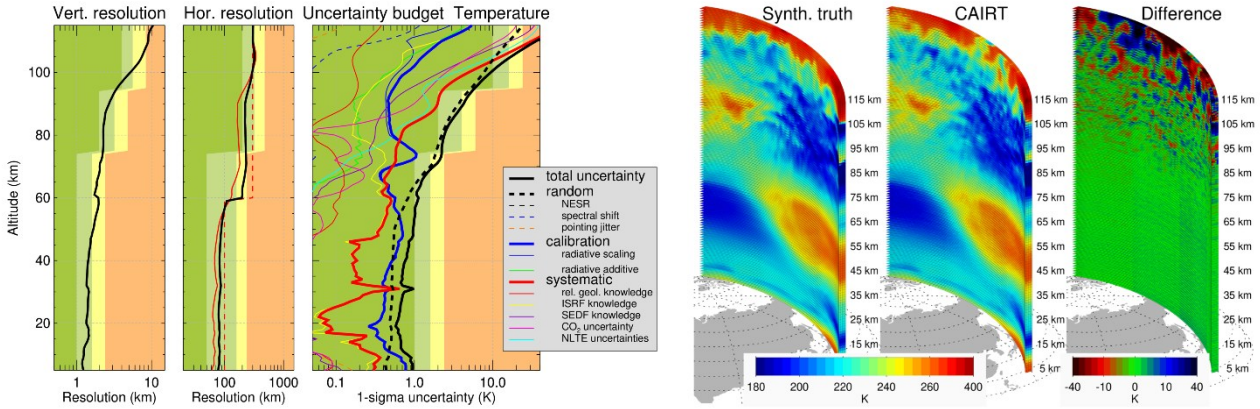

Figure 11: L2a Performance estimation for temperature for Concept B. Detailed caption provided in Figure 10.

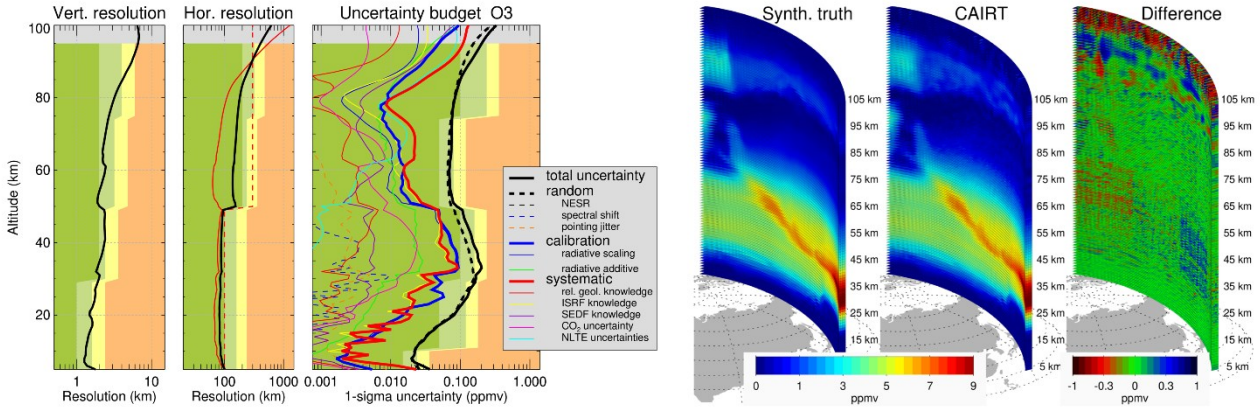

Figure 12: Performance estimation for ozone for Concept A. Detailed caption provided in Figure 10.

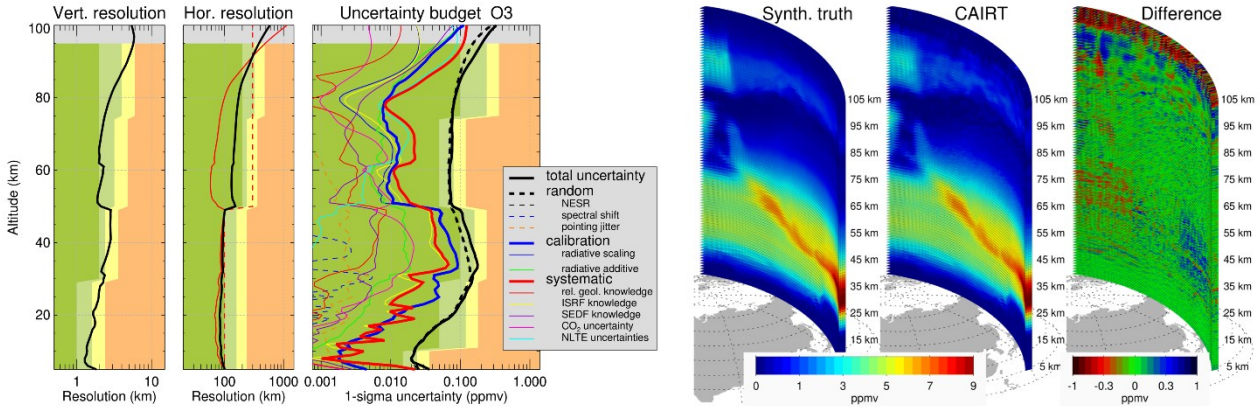

Figure 13: Performance estimation for ozone for Concept B. Detailed caption provided in Figure 10.

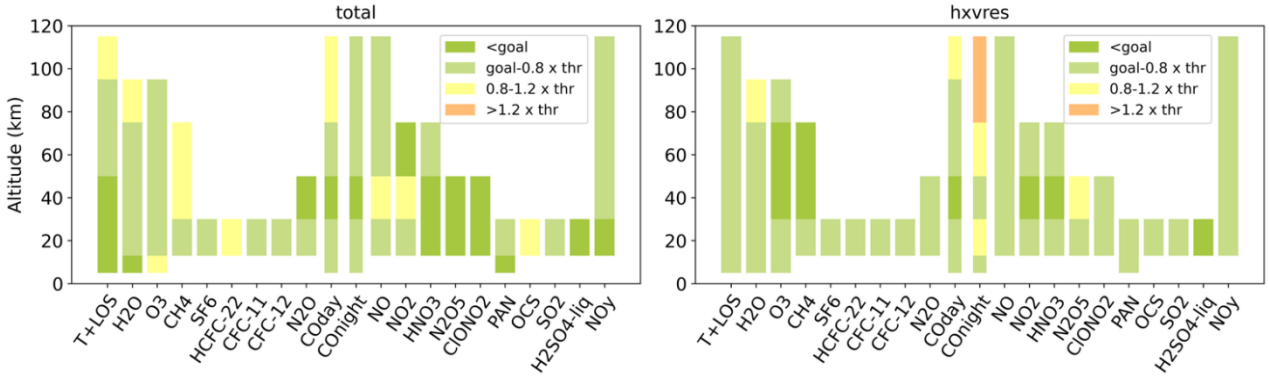

Figure 14: Retrieval performance assessment overview plot for all primary L2a targets and NOy, for Concept A. Left, estimated total uncertainty/error; right, spatial resolution (hxvres). Colours (see Table 2) correspond to the evaluated averaged performance (over ERS and regions), against goal and threshold geophysical requirements.

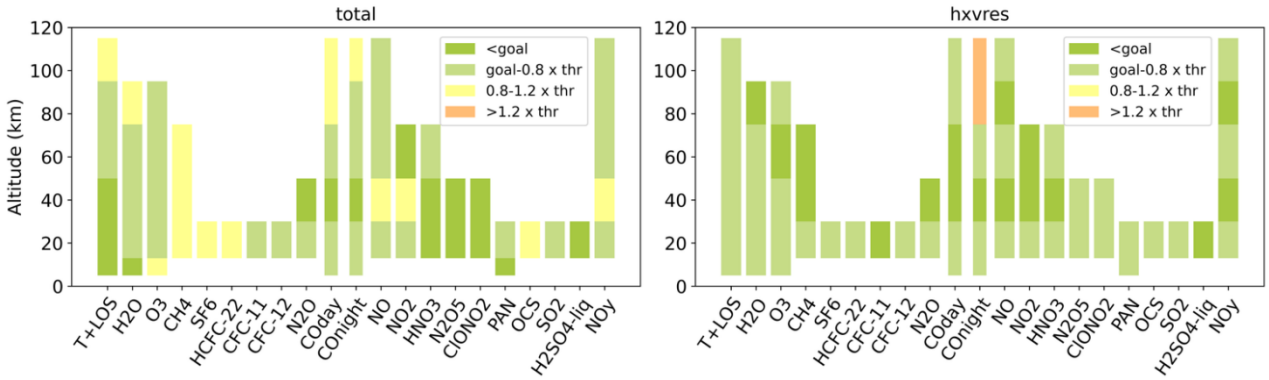

Figure 15: Same as Figure 14 but for Concept B.

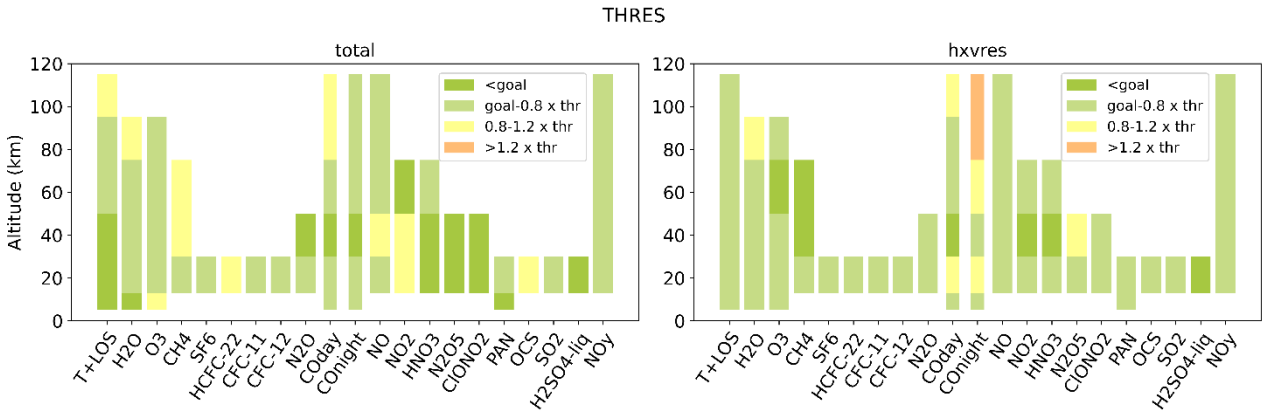

Figure 16: Same as Figure 14 but for requirement threshold.

The performance of the L2b products for AoA and gravity-wave (GW) parameters has been systematically evaluated using the SWB. In particular, the L2b AoA retrieval capability is assessed using L2a trace-gas fields simulated with the FL2S forward simulation system, following the prescribed AoA test scenario TDS-G-05 (**Table 3**) and assuming threshold-level performance for the L1b radiance measurements.

The evaluation is conducted for a one-day period using zonal-mean diagnostics, with the model's artificial "clock tracer" serving as the reference truth for AoA. This framework allows a direct comparison between (i) the AoA uncertainty obtained from retrieval-propagated errors and correlation-based estimates, and (ii) the actual retrieval error diagnosed against the clock-tracer truth.

AoA is derived from the suite of trace-gas distributions produced by FL2S along the satellite orbit tracks and subsequently aggregated into zonal-mean fields (**Figure 17**a). These retrieved zonal means are contrasted with corresponding zonal-mean clock-tracer values, yielding a quantitative estimate of the systematic bias (**Figure 17**b). In parallel, differences between retrieved and true AoA are computed at the native along-track sampling. The standard deviation of these differences, evaluated in selected latitude–altitude bins, provides a measure of the random retrieval error and of the instrument's ability to resolve small-scale structures such as stratospheric filaments and transport barriers (**Figure 17**d). The bias (panel b) and standard deviation (panel d) are combined in quadrature to produce a total root-mean-square (RMS) error (**Figure 17**e).

By contrast, **Figure 17**c displays the AoA uncertainty obtained solely from the retrieval chain. This estimate incorporates both the propagated uncertainties from individual trace-gas retrievals—treated as statistically independent—and the additional correlation-method uncertainty resulting from imperfect trace-gas–AoA relationships. A comparison of the retrieval-based uncertainty (panel c) with the diagnosed RMS error (panel e) reveals close agreement in both spatial structure and magnitude. This concordance indicates that the employed error-propagation and correlation framework reliably captures the dominant error sources affecting the AoA retrieval. Importantly, the total AoA uncertainty remains better than the mission threshold requirement of 0.5 years throughout the full vertical domain considered, demonstrating robust L2b performance under nominal conditions.

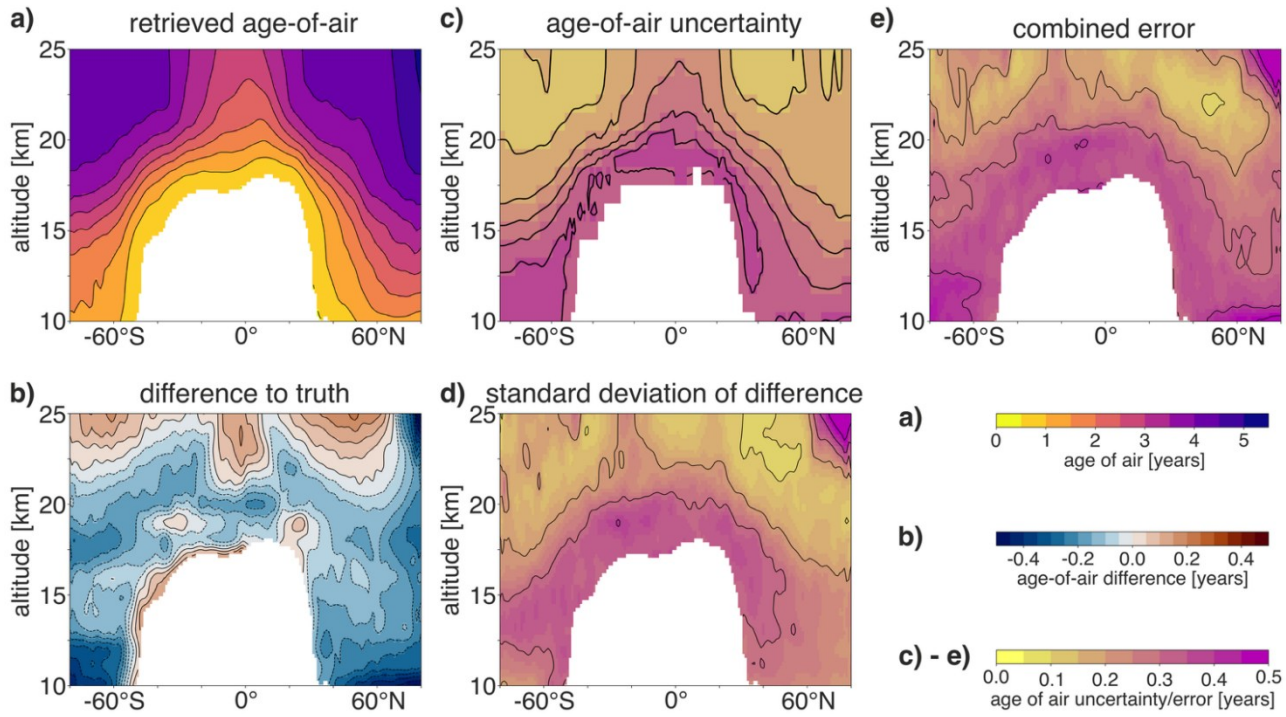

Figure 17: Performance evaluation of AoA derived with the correlation method from synthetic CAIRT observations, accounting for retrieval uncertainty and simulated observation errors: a) retrieved AoA; b) deviation of the retrieved AoA from the clock-tracer AoA; c) uncertainty estimate propagated from the uncertainties of the individual tracers; d) standard deviation of the differences between retrieval and truth; e) combined error, defined as the root-mean-square of (b) and (d).

Performance of the L2b GW parameter products is evaluated using a dedicated processing chain that integrates both the atmospheric retrieval and subsequent GW analysis. This evaluation is conducted for GW scenario A (**Table 3**, TDS-G-03a), under the assumption that the L1b data meet their threshold performance requirements. Differences between the Monte-Carlo realisations and the corresponding reference fields are quantified by computing the standard deviation at each altitude level and within 30° latitude bands, as illustrated in **Figure 18**. The colour scale is chosen to reflect the scientific requirements and to be consistent with the performance metrics (**Table 2**). The goal performance is achieved throughout the 30–60 km altitude range, and the threshold performance is satisfied for most GW-related parameters across the full altitude domain of interest (20–80 km).

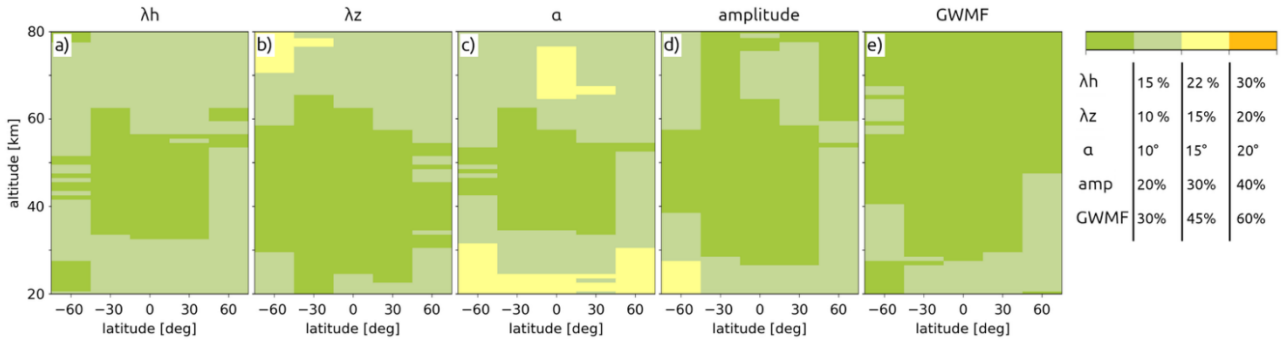

Figure 18: Uncertainty estimates for individual-wave parameters. Zonal-mean standard deviations, computed in 30° latitude bands, of (a) vertical wavelength, (b) horizontal wavelength, (c) wave direction, (d) amplitude, and (e) absolute GW momentum flux (GWMF).

6 Tasks 7 and 8: Impact studies for scientific applications and the potential for societal impact

6.1 Impact Study 1 to constrain age-of-air

Changes in the large-scale Brewer-Dobson circulation (BDC) will have a direct impact on the distribution of the ozone layer, the intrusions of stratospheric ozone into the troposphere and the water vapour distribution in the UTLS, among others, with important implications for Earth's climate. The strength of the BDC is estimated with the concept of AoA. AoA is defined as the average time an air parcel from tropospheric origin spent in the stratosphere. AoA can be modelled using an idealised inert clock tracer with constant surface emission. In the natural environment, AoA can be estimated from observations of long-lived trace gases exhibiting a monotonous increase in their surface mixing ratios, as has been done with in situ balloon measurement of CO_2 and SF_6 since the mid-1970's. Current models predict an acceleration of the BDC while observations suggest the opposite, although these are not statistically significant due to large uncertainties in the small number of observations (see e.g., Chabrillat et al., 2018; Garny et al., 2024; Ploeger et al., 2019). **Figure 19** shows the monthly zonal mean AoA from the Belgian Assimilation System for Chemical ObsErvations (BASCOE) model simulations estimated from an inert model clock tracer and driven by three meteorological reanalyses,. It is evident that reanalyses disagree by significantly more than 0.25 years, which is too large to diagnose changes in the BDC. disagree by significantly more than 0.25 years, which is too large to diagnose changes in the BDC. disagree by significantly more than 0.25 years, which is too large to diagnose changes in the BDC.

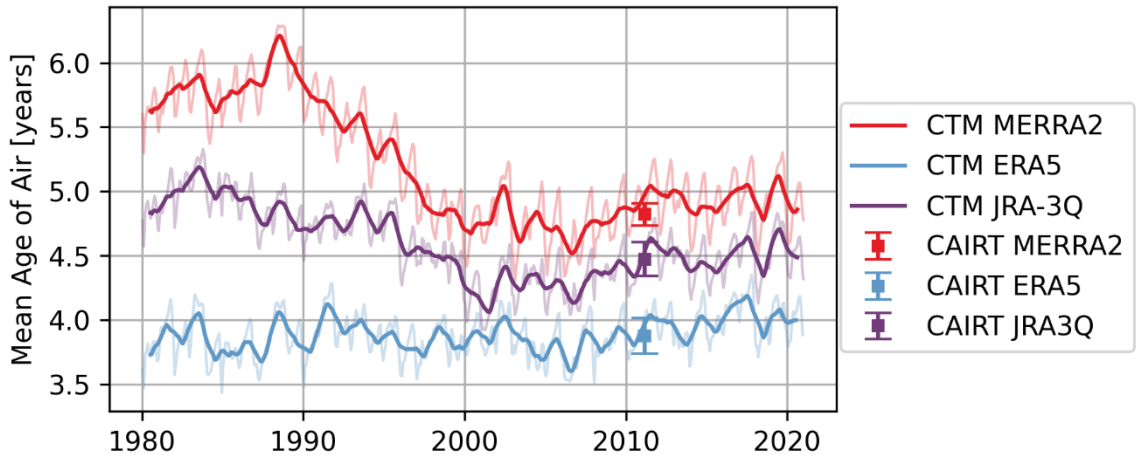

Figure 19: Time evolution of AoA averaged at 25 km altitude and for northern mid-latitudes (40–50°N). Thin coloured lines show the monthly zonal mean AoA from BASCOE model simulations driven by three meteorological reanalyses, estimated from an inert model clock tracer. Solid coloured lines show the 1-year running mean of the monthly BASCOE AoA. Squares represent CAIRT L2b AoA zonal mean values simulated for 1 February 2011, from BASCOE simulations of stratospheric composition driven by the same three reanalyses, using FL2S and the Voet et al. method to calculate AoA. Error bars around CAIRT values represent 1σ of the standard deviation.

The CAIRT capability to observe AoA with unprecedented small total uncertainty will enable tying these differences to specific parametrisations in the different reanalyses or models. Using three additional BASCOE model simulations driven by the same three reanalyses, CAIRT synthetic AoA observations were simulated, then averaged, and added to **Figure 19**. In these simulations, BASCOE included detailed stratospheric chemistry of SF_6, CH_4, N_2O, CFC-11, CFC-12 and HCFC-22, and was run for the 1997-2020 time period (Vervalcke et al., 2026). Synthetic observations were generated from the model along a simulated CAIRT day (Feb. 1, 2011) using FL2S to account for spatial resolution and total uncertainty of CAIRT L2a products. From

these, AoA profiles were calculated using the L2b algorithm implementing the method described by Voet et al. (2025). Averaged over one day, these synthetic L2b profiles give the CAIRT data points shown in **Figure 19**. The attached error bar provides the 1σ standard deviation of the data. Overall, CAIRT AoA values have a small uncertainty that is much lower than the AoA differences between the different reanalyses or balloon observation errors shown e.g. by Engel et al. (2017). Although these results must be confirmed by using additional dates, this small uncertainty of CAIRT AoA data will allow assessing and constraining the BDC's representation in reanalyses, and more broadly in models in general. More details maybe find in (Errera et al., 2025b). This study is also expected to be consolidated and published by S. Vervalcke in the CAIRT special issue.

6.2 Impact Study 2 for consistent simulation of the dynamic driving and trace species impact of a sudden stratospheric warming

Sudden stratospheric warmings (SSWs) are one of the most dramatic events occurring in the middle atmosphere. Over just a few days the entire polar stratospheric vortex breaks down. This can have dire consequences for surface weather as, for instance, the SSW-induced cold air outbreak in February 2018 – often referred to as the "Beast from the East" – shows. During this event snow hit many unprepared communities along the Mediterranean coast, across Europe and in the UK. But SSWs can also have an important impact on mesosphere-to-stratosphere coupling. In our study we focus on the SSW of 2018/2019 which developed an elevated stratopause (ES) with strong downward transport of reactive nitrogen in the mesospheric polar vortex, showcasing the full potential of CAIRT in the entire middle atmosphere.

The study consists of two parts. In the first part, ECMWF operational analysis data covering December 2018 to March 2019 were used to generate synthetic CAIRT observations of GW parameters in the stratosphere. ECMWF data are known to contain almost the entire GW spectrum visible for CAIRT. The data were used to demonstrate the potential of CAIRT for identifying GW sources and show differences in the wave driving before and after the central date of the SSW (Rhode, 2025). An animation of GW raytracing highlights the distance the GWs propagate from source to observation altitude (https://doi.org/10.5281/zenodo.17275660).

For the second part, the WACCM-X model was nudged to different meteorological data sets, which have different capabilities to resolve GWs. MERRA data resolve only very long scale GWs. Thus, nudging to this data set strongly suppresses waves, which the free-running WACCM would contain. Realistic wave driving can be reached by nudging to ERA-5, which contains GWs down to about 200 km horizontal wavelength, compatible to what WACCM natively resolves. This still leaves a supposedly major short-scale part of the GW spectrum unresolved. However, adding a GW parametrization to account for this missing part results in highly exaggerated drag. In the following, these three cases will be referred to as "weak" (MERRA), "moderate" (ERA-5 w/o parametrization) and "strong" (ERA-5 w/ parametrization). The SSW-ES event was also observed by the SABER IR limb sounder. The temporal development of the observed elevated stratopause shown in **Figure 20** is used to judge whether the simulated wave driving is realistic (the only possible diagnosis without having available real CAIRT observations of GW parameters).

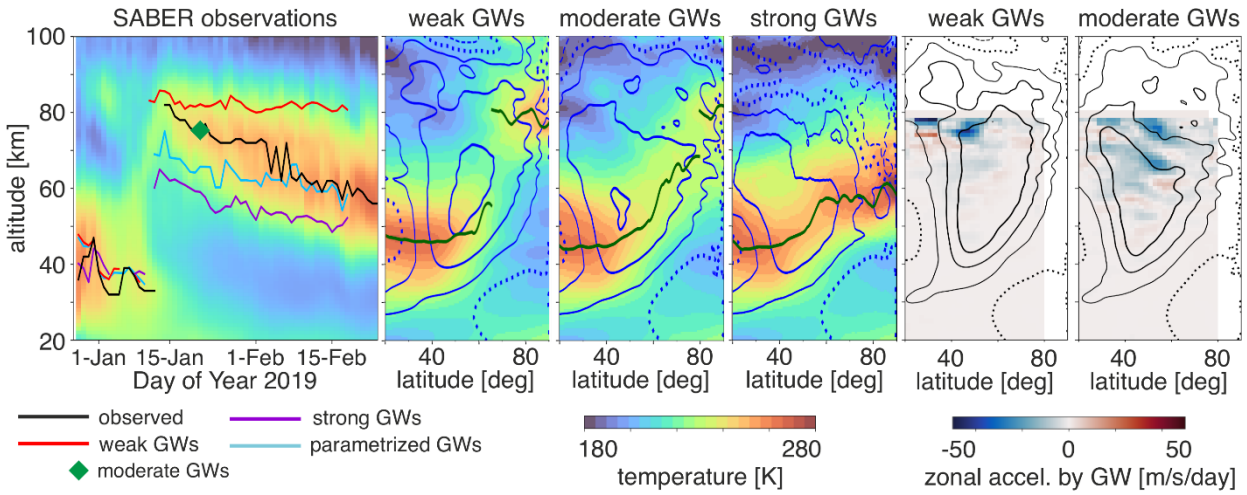

Figure 20: Impact of different GW representations in the WACCM-X model and observed reality (a) Temperature time series from TIMED/SABER temperature observations at 70–85° N and the inferred stratopause (black line) compared to the simulated stratopause heights from various GW drag realizations in the WACCM-X model (colored lines and diamonds); (b, c, d) WACCM-X model zonal mean temperatures and zonal winds (solid contours: eastward at 20, 50, and 100 m/s; dotted: zero wind; dashed: westward) on January 21 (diamond in the left panel), with the stratopause shown as a dark green line; (e, f) GW drag from synthetic CAIRT observations that led to these temperature distributions.

Where the GWs break, they induce drag and slow down the background flow. Too weak drag maintains the vortex at elevated levels for an unrealistically long time, while too strong drag destroys the vortex above 70 km entirely. CAIRT, however, would directly provide GW drag up to approx. 80 km altitude and can discern between these two drag situations by inferring it directly from L2b products. CAIRT's ability to directly observe the drag allows for detailed investigations of SSW dynamics and reliable constraints to GW parameterizations in climate models.

The GW-induced large-scale dynamics is closely linked to trace species transport in relation to space weather: NO produced in the lower thermosphere is transported by the meridional circulation to the stratosphere during polar winters. This transport is strongly enhanced in the aftermath of an SSW which is followed by an ES event. CAIRT observations allow to discern the effects of different GW implementations in the WACCM-X model simulations of the 2019 SSW-ES event on NO transport from the lower thermosphere. This is demonstrated by simulating CAIRT observations for the "weak" GW case, as discussed in the previous section. In order to quantify the impact of different GW implementations, we compare the zonally averaged NOy in the NH polar region with a parametrized GW simulation. The simulated CAIRT data reproduce the descending NOy "tongue" of the "weak" GW model simulation with high fidelity. In contrast, the parametrized GW simulation shows the tongue forming at much lower altitudes, accompanied by less descending NOy because of the lower altitude of the polar vortex. This prevents efficient subsidence into the mesosphere. CAIRT observations clearly distinguish the temporal evolution of the different GW cases and give insight into the physical processes.

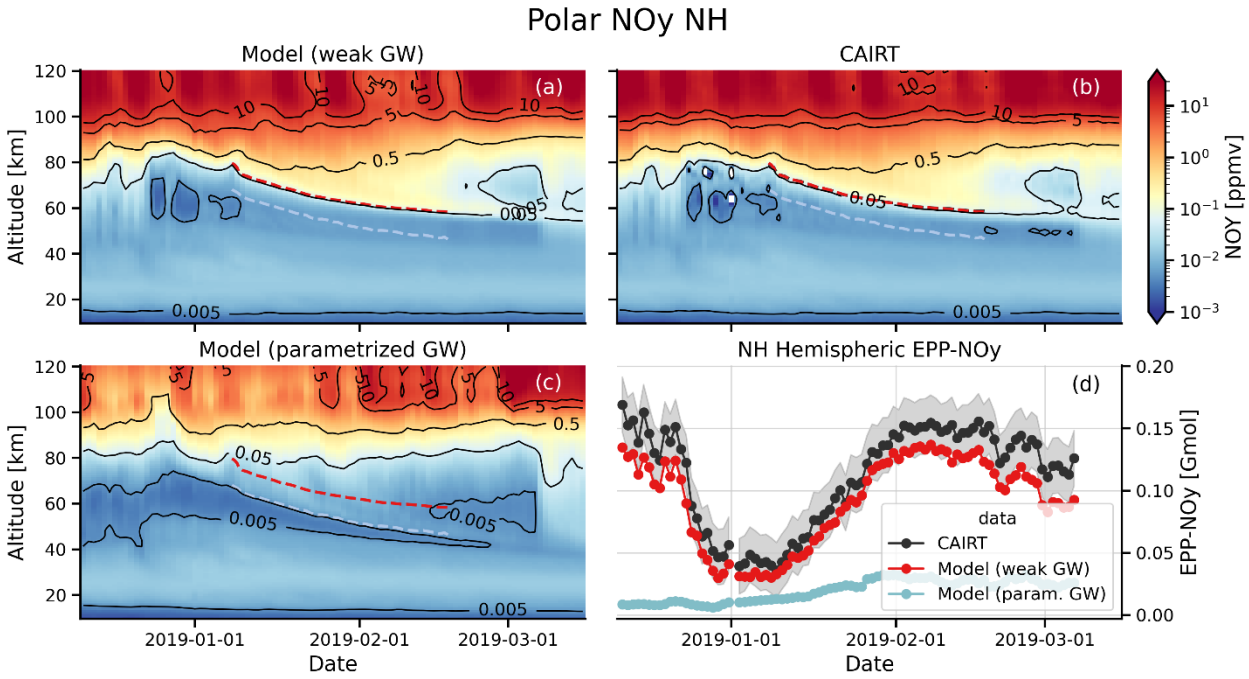

Figure 21: Temporal evolution of zonally averaged NOy at 70-90°N throughout the SSW-ES episode from a model simulation with (a) "weak" GW drag and (c) "parametrized" GW drag. (b) Same as (a) but for CAIRT synthetic data from the weak GW model "truth". (d) Temporal evolution of the hemispheric EPP-NOy amount descending below 70 km for the weak GW model "truth", the CAIRT data (CAIRT), and the parametrized GW model simulation.

6.3 Impact Study 3 on geoengineering via stratospheric sulfur injection

To cope with the observed anthropogenic climate change and its effects, stratospheric aerosol geoengineering (SAG) has been proposed as a complementary solution together with mitigation, adaptation, and carbon dioxide removal. Mimicking extreme volcanic eruptions, in SAG techniques sulphur dioxide (SO2) is injected into the stratosphere with the aim of forming highly reflective and small-sized sulphate aerosol (SA) particles. These can effectively scatter back a part of the incoming solar radiative flux to counterbalance the reduction of outgoing longwave fluxes associated with the increase of greenhouse gas concentrations from anthropogenic emission. Several, unwanted side effects are expected in case of deployment of SAG techniques, such as a thinning of the stratospheric ozone layer delaying the recovery from the Antarctic ozone hole phenomenology. We have investigated the expected capability of the Earth Explorer 11 candidate mission CAIRT to detect SAG interventions and their impacts on the stratospheric aerosol and ozone layer.

Geo-engineering SAG scenario pseudo-realities (PR) are obtained using simulations from the WACCM version 6, as described by Tilmes et al. (2020). All the modelling experiments used in this work are realised in the context of the Coupled Model Intercomparison Project, Phase 6 (CMIP6) action, and are based on the Shared Socioeconomic Pathway 5 - Ozone Scenario – 3.4 (SSP5-OS-34) "overshoot" social development pathway (O'Neill et al., 2016). Based on the SSP5-34-OS baseline, modelling experiments are realised to account for an additional SAG deployment in this scenario (Geo SSP5-34-OS 2.0: SAG deployed with the aim of limiting the global temperature increase to 2.0°C above 1850–1900 conditions). Based on these PR scenarios, we produced SO_2, sulphate aerosol (SA) and ozone CAIRT pseudo-observations (PO) using a two-step processing chain: first we projected the PR over a retrieval grid representing a full day of CAIRT observations and then we applied representative vertical smoothing and noise and systematic error using the FL2S simulator.

Our results suggest that CAIRT will be able to detect and quantify the mass of SO_2 injections, and to locate their horizontal and vertical injection position, even when these are the very weak initial injections in our PR scenario (e.g. the first injection in the PR scenario, in January 2034, see **Figure 22**). These injections are of the

order of magnitude of a few to a few tens tons SO_2, which is characteristic of "near-term" to "mid-term" experiments, i.e. scenarios considered feasible even unilaterally/illegally with presently existing technology and relatively low cost. In addition, our results suggest that CAIRT will be able to track the temporal evolution of the subsequently formed reflective SA, as it spreads toward higher latitudes through meridional dispersion, as well as monitor changes in its vertical distribution over time. Processes like the self-lofting of the resulting SA plume, due to diabatic heating by radiation absorption, is also well characterised with CAIRT PO. Finally, our results suggest that CAIRT will be able to detect and characterise the impacts of SAG interventions to the stratospheric ozone layer, and in particular, the delayed ozone hole recovery at southern-hemispheric high-latitudes, as well as its seasonal cycle.

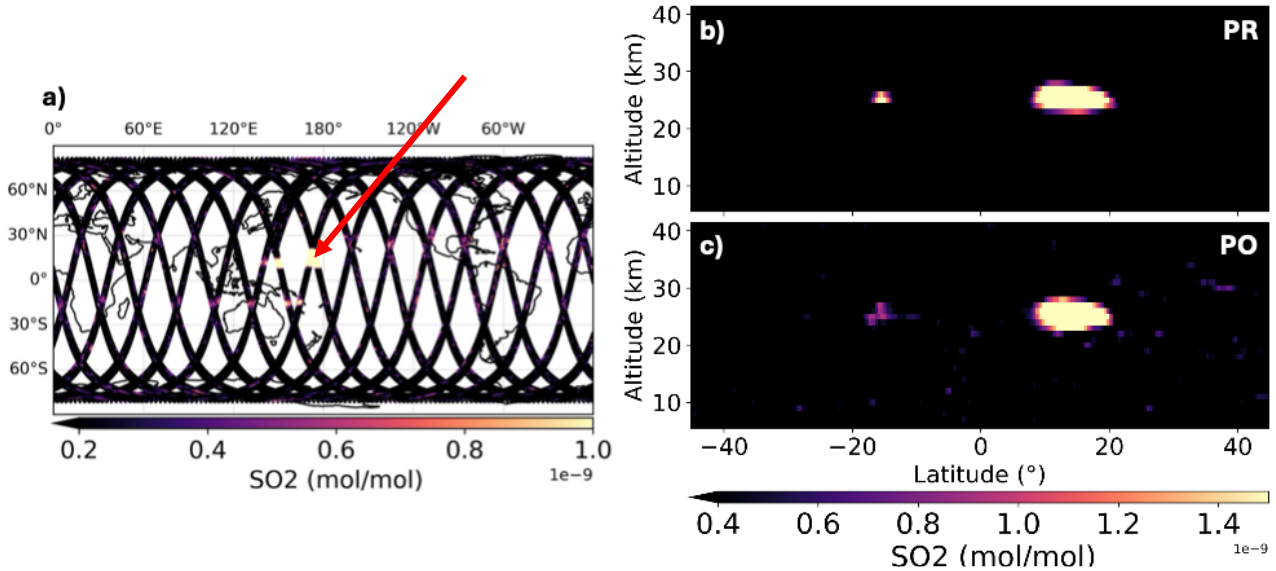

Figure 22: (a) CAIRT PO of the SO_2 concentration for February 2034, at 25 km altitude. (b-c) Average PR (panel b) and CAIRT PO (panel c) of the SO_2 vertical profiles, for the orbit individuated with a red arrow in panel a.

6.4 Impact Study 4: Observing System Simulation Experiment ozone and water vapour

The UTLS is an essential region for the Earth's radiative balance, which is strongly influenced by the sharp gradients in greenhouse gases that characterise this interface layer. Model studies have shown that the radiative effects of ozone and water vapour in the UTLS are particularly sensitive to the representation of atmospheric mixing (Riese et al., 2012). Resolving mixing, the sharp vertical gradients and tracer fluxes in the UTLS and across the tropopause is thus essential for better understanding the links between (changing) UTLS composition, dynamics, radiation and climate.

A recent evaluation of the impact of the limb sounder Microwave Limb Sounder (MLS) water vapour profile assimilation on ECMWF analyses and weather forecasts has identified reductions in the UTLS water vapour moist bias and temperature cold bias, with significant improvements of weather forecasts at all lead times (Semane and Bonavita, 2025). This moist bias in the lowermost stratosphere and the associated cold bias are a common feature of almost all NWP and climate models (Charlesworth et al., 2023), impacting sub-seasonal-to-seasonal predictions (Lawrence et al., 2022). In addition, lack of ozone representations in NWP systems also leads to stratospheric temperature biases (Monge-Sanz et al., 2022). CAIRT is expected to significantly contribute to reducing such biases, which could translate into substantial improvements to predictive skill.

The capability of CAIRT to reproduce gradients and variability in the UTLS was evaluated with an Observing System Simulation Experiment (OSSE) targeting ozone and water vapour (Errera et al., 2025a). OSSEs

evaluate the added value of potential instrument(s) by using simulated observations and data assimilation. A nature run (NR) defines the reference state of the atmosphere from which observations are simulated, and a control run (CR) provides the baseline atmospheric state. An assimilation run (AR) of the simulated observations allows quantifying the added value of the new instrument as compared to NR and CR. To avoid the "identical twin" problem leading to overoptimistic results, the AR and CR should use a different model compared to the NR.

Building on preliminary CAIRT Phase 0 work, the OSSE was extended (i) from a period of two to five months – now covering October 2021 to February 2022, (ii) by including H_2O in addition to O_3, and (iii) by using a consolidated representation of CAIRT threshold performance. The relatively high spatial resolution of a Copernicus Atmosphere Monitoring Service (CAMS) operational control simulation (~40 km horizontal, <500 m vertical in the troposphere with 3-hourly output), without chemical data assimilation, was used as NR (Schoenhardt et al., 2023). CAIRT profiles of O_3 and H_2O were generated by interpolating CAMS outputs in time and space to a simulated CAIRT orbit and applying the FL2S; in other words, by convolving with CAIRT averaging kernels, and adding perturbations representative of CAIRT random and systematic errors.

Profile segments below clouds were discarded where CAMS cloud fraction exceeds 0.2. MLS observations were also simulated and assimilated to evaluate the added value of CAIRT against a key reference instrument providing limb observations of O_3 and H_2O. These profiles were simulated using the existing geolocation of MLS profiles, the retrieved L2 error profiles and averaging kernels, and the MLS quality flags of L2 profiles. Control and assimilation runs use the BASCOE system (Errera et al., 2021).

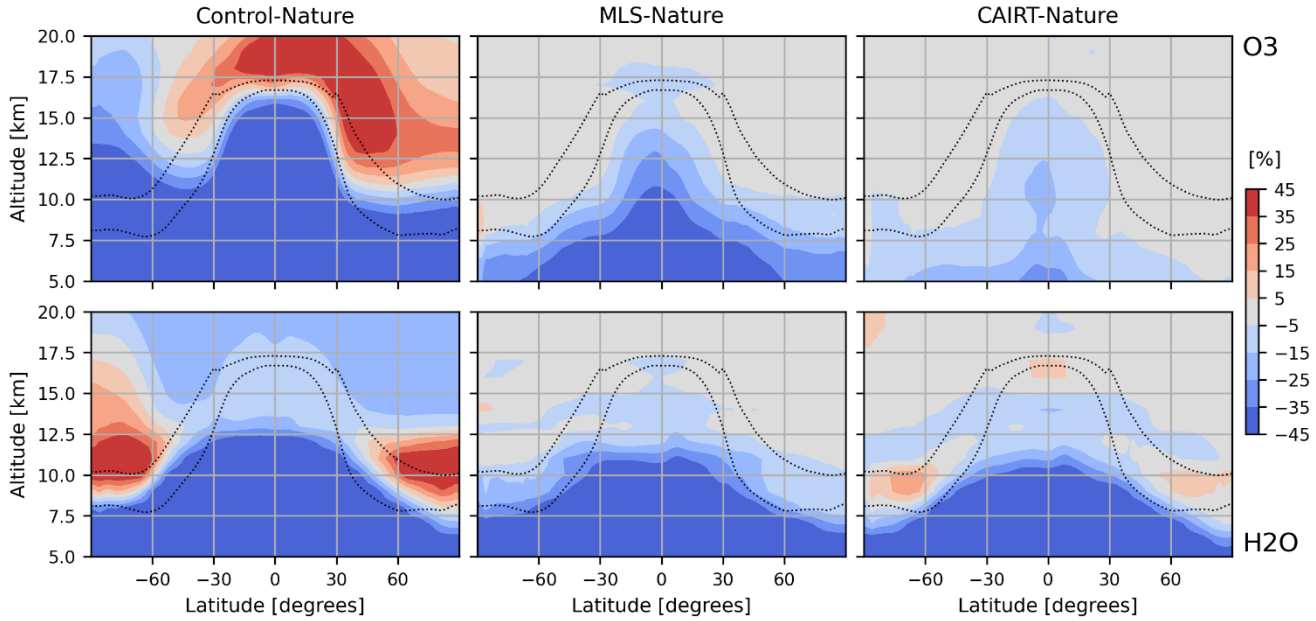

Figure 23: Top, CAIRT OSSE results for O_3 showing the zonal mean difference between (from left to right) the Control run, MLS run, CAIRT run, and the Nature run for the period October 2021 to February 2022. Bottom, same as top row but for H2O. The dashed lines represent the thickness of the tropopause during the specified time frame.

Figure 23 compares the performance for O_3 and H_2O of the CR, and of the two ARs against NR. As expected, this OSSE suggests that CAIRT, like MLS, would successfully eliminate the bias in the stratosphere. Less expected was the constraint by CAIRT that allows to largely reduce the O_3 negative bias in the troposphere down to 7 km of altitude compared to the control run, which is an improvement over MLS. For H_2O, CAIRT and MLS have comparable benefits in the upper troposphere, reducing the dry bias in control run.

Improvements are not limited to the reduction of the preceding climatological bias. CAIRT is also expected to help improving the representation of O_3 and H_2O for specific situations (**Figure 24**). The ozone distribution

shown at 7 km during a tropopause fold above Europe is well represented by CAIRT and MLS runs, correcting for the bias in the control run. CAIRT data largely reduces the negative bias of the control run outside the tropopause fold region and does so to a larger extent than MLS data. CAIRT ozone observations in the UTLS will contribute to diagnosing stratosphere-to-troposphere transport, which may intensify in a strengthening BDC.

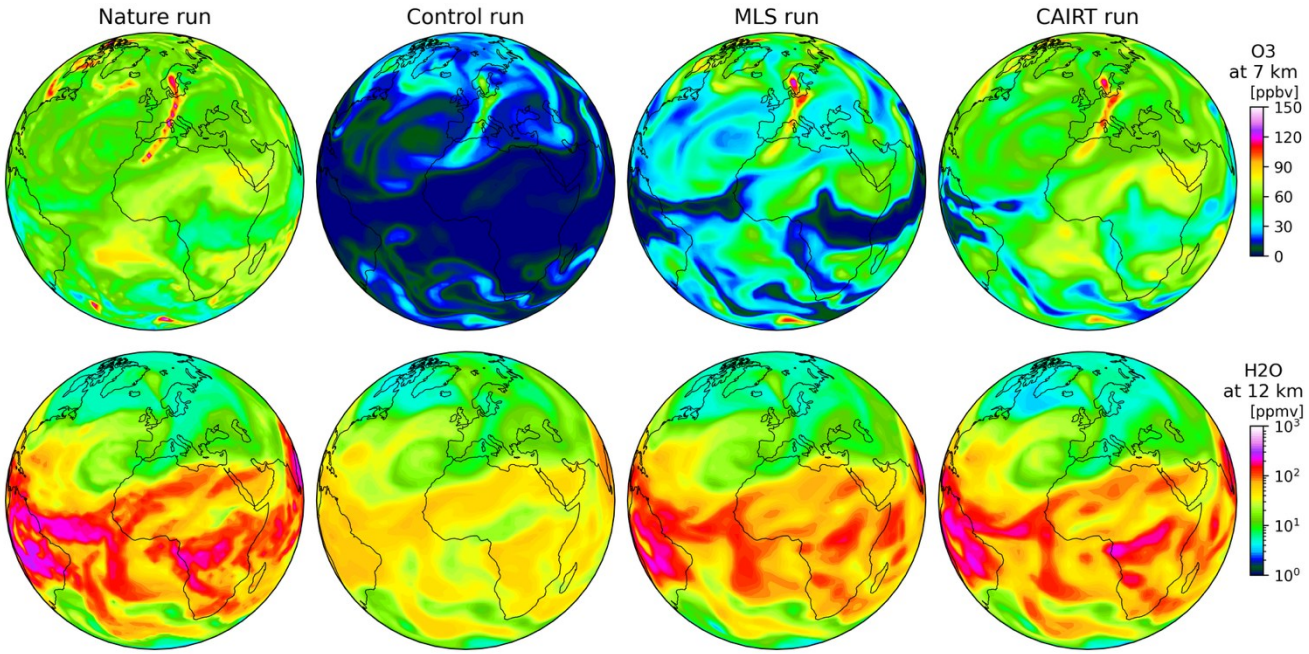

Figure 24: Top, O3 distribution [ppbv] at 7 km of altitude on 3 December 2021 at 0:00 UTC for (from left to right) the Nature run, the Control run, the MLS assimilation run and the CAIRT assimilation run. Bottom, same as top row but for H2O at 12 km of altitude.

Similarly, CAIRT observations provide a significant constraint in the representation of water vapour at 12 km, which is equivalent to that of MLS. The OSSE demonstrates that CAIRT water vapour observations in the lower stratosphere will provide essential data that is likely to significantly improve NWP. As mentioned above, the value of UTLS limb sounding and of reintroducing operational data assimilation of stratospheric humidity for improved NWP forecast skill in the medium and extended range has recently been highlighted after initial efforts that date back over 20 years (Semane and Bonavita, 2025). Additional sensitivity tests assessing the impact of CAIRT systematic errors, cloud coverage, and reduced swath width are described in Errera et al. (2025a).

6.5 Impact Study 5 on stratospheric composition for weather and climate prediction

Insufficient information on stratospheric processes in most NWP models is linked to an unrealistic representation of stratosphere–troposphere coupling, which renders most existing models unable to exploit stratospheric sources to improve surface meteorological predictions (Scaife et al., 2016).

The links between stratospheric composition, stratospheric circulation and polar vortex dynamics are being increasingly recognised as a source of improvement for extreme weather and seasonal climate predictions over Europe and the North Atlantic sector (e.g. Monge-Sanz et al., 2022; Scaife et al., 2022). Winter extreme cold events in Northern mid and high latitudes are often linked to atmospheric disruptions originating in the stratosphere. How realistically NWP models simulate these events, their coupling with radiative chemical

species and their downward propagation is essential to improve prediction of these winter cold snaps at surface level.

This impact study highlights the need of CAIRT-like observations and their spatial resolution to better resolve the UTLS and the stratosphere regions, both crucial for utilizing upper atmospheric sources to improve surface meteorological predictions. For this, we have performed simulations with the world-leading recognized weather prediction model of the ECMWF. In these simulations we have assessed the impact of using limb sounding observations of ozone, the stratospheric chemical species most relevant for interaction with temperature and winds. Our simulation experiments cover several month periods for selected Northern Hemisphere winters within the overall period 2020-2023.

Figure 25 shows the difference in mean temperature for two simulations with identical model configurations, except that one of them assimilates MLS ozone profiles and the other one does not. Radiative effects cause changes in the mean temperature between these two simulations, especially in the stratosphere and the tropopause regions but the signal also goes down to the troposphere and surface levels at mid and high latitudes. The simulation period corresponds to Northern Hemisphere winter 2021, when surface temperatures were affected by stratospheric disruptions.

Our results show that assimilating limb observation profiles of ozone improve stratosphere and UTLS temperature and winds in numerical weather prediction simulations. Our simulations used the ECMWF model version used for operational weather prediction during 2024-2025, with CAMS configuration for the assimilation of chemical species. Therefore, our results also show the potential of limb observations of middle-atmosphere chemistry for Copernicus datasets.

Similar differences to the ones shown in **Figure 25** have also been found in a recent study with MLS H_2O assimilated in experiments with the ECMWF operational system (Semane and Bonavita, 2025). Such differences corresponding to assimilation of MLS H_2O were similar in nature although smaller in amplitude, and yet such study has prompted ECMWF to the decision of assimilating MLS H_2O in their NWP operational forecasts. Suitable alternatives to MLS are therefore needed to provide the same or improved gain of information after the planned decommission of the MLS satellite instrument. For stratospheric species, CAIRT would improve the level, amount and quality of information MLS can provide for NWP applications.

More details about this Impact Study can be found in the CAIRT PerReC Phase A deliverable DEL-15-5-TR2.5-CAIRT-PhAPerReC, which is the basis for a publication in preparation for the ACP Special Issue/Collection.

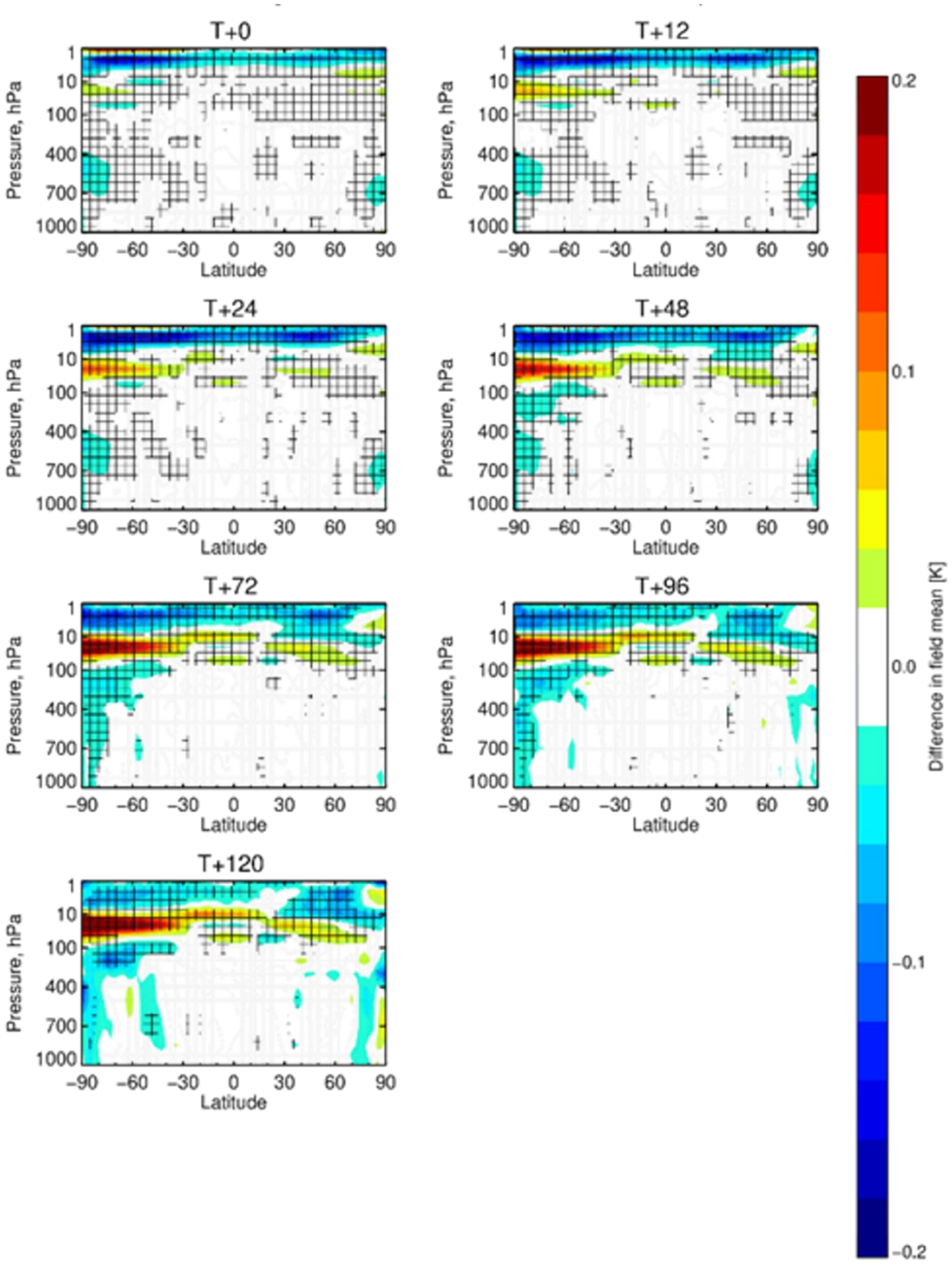

Figure 25: Altitude-latitude distribution of differences in the mean temperature field between two ECMWF model simulations covering the period December 2020 – March 2021. Both simulations use identical model configuration except that one of the simulations does not assimilate MLS ozone data. Each panel corresponds to a different forecast lead-time, from 0h (day 0) up to 120h (day5) from the forecast initialisation. Hatched regions indicate those regions where the change in temperature is statistically significant at the 95% confidence level.

6.6 Impact Study 6 for volcanic ash detection

Ensuring flight safety during volcanic eruptions increasingly depends on our ability to monitor, in near-real time, both the vertical structure and the composition of volcanic clouds. Events such as the 2010 Eyjafjallajökull eruption and recurrent eruptions of Mount Etna clearly demonstrate the vulnerability of aviation to volcanic ash and highlight the need for accurate, timely information on the distribution of volcanic aerosols. The motivation for this study therefore stems from the requirement to substantially improve the tools available for detecting, characterizing, and forecasting volcanic ash clouds.

Current observation systems offer only a partial solution. Geostationary nadir-viewing instruments—such as MSG-SEVIRI—can provide estimates of ash column abundance with global coverage and revisit times shorter than 15 minutes. However, despite their excellent spatial and temporal coverage, these sensors cannot determine either the altitude or the thickness of volcanic clouds, which are essential parameters for assessing the hazard to aviation. Lidar systems, on the other hand, can retrieve cloud thickness with high vertical resolution; yet space-borne lidars suffer from low spatial and/or temporal resolution (e.g the two EarthCARE active instruments collect vertical profiles only for the satellite track), while ground-based systems are limited by very sparse spatial coverage. As a result, no existing observational technique can provide, on its own, the full set of information required for effective volcanic cloud monitoring.

In this context, the CAIRT mission introduces a new capability. CAIRT can simultaneously retrieve the altitude, vertical extent, and horizontal distribution of volcanic clouds, enabling a more accurate characterization of volcanic ash concentration and plume evolution. Sensitivity tests conducted within this study confirm that CAIRT is responsive to the presence of clouds and can distinguish, under specific particle size and density conditions, between ice and ash. Moreover, the cloud indices developed by Griessbach et al. (2014) have been shown to be applicable to CAIRT observations, offering additional diagnostic potential.

A key component of the analysis focuses on CAIRT's ability to detect volcanic ash originating from moderate-intensity eruptions. To investigate this, we simulated the 23 November 2013 Etna eruption using the Weather Research and Forecasting (WRF) with Chemistry model (WRF-Chem) (Grell et al., 2005), which includes an advanced module for the emission, transport, and deposition of volcanic aerosols (Stuefer et al., 2013). The resulting atmospheric fields were projected onto CAIRT's retrieval grid and used to generate synthetic spectra: CAIRT-like spectra through the GBB-clouds model (Castelli et al., 2011) and SEVIRI-like spectra through the σ-IASI/F2N model (Masiello et al., 2024). Nadir-viewing synthetic measurements were included to evaluate whether the total ash concentration can be retrieved from using the columnar abundance routinely obtained from geostationary satellite data and the information on the geometrical thickness of the cloud coming from CAIRT observations.

The results, summarized in **Figure 26**, highlight CAIRT's significant added value. On the left, the WRF-Chem ash plume subsampled onto the CAIRT grid is shown alongside the corresponding CAIRT cloud-extension retrieval (in red). On the right, the ash density is retrieved using combined SEVIRI and CAIRT measurements through the Volcanic Plume Retrieval (VPR) approach (Guerrieri et al., 2015). The figure clearly demonstrates CAIRT's ability to accurately determine the top height, thickness, and horizontal extension of ash clouds. Remarkably, when multiple cloud layers occur at different altitudes, CAIRT can resolve them separately, something that nadir-viewing instruments cannot achieve.

Overall, this study demonstrates that CAIRT:

- accurately resolves the horizontal and vertical structure of clouds, regardless of particle type,
- can distinguish ash from ice clouds for particles smaller than 3.5 μm,
- is sensitive to thin or optically thin clouds that remain undetectable from nadir-viewing instruments,
- supports improved retrievals of ash concentration when combined with existing geostationary observations.

These results show that CAIRT can fill key observational gaps and provide critical information for real-time volcanic ash monitoring and aviation safety. By complementing the limitations of current systems, CAIRT represents a major advancement in the global capability to detect, characterize, and forecast the evolution of volcanic clouds.

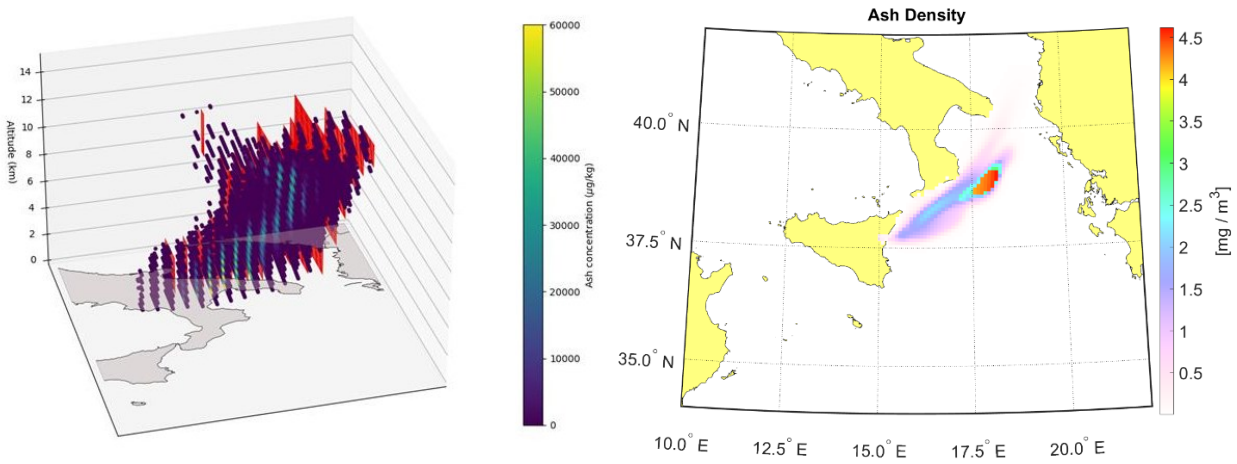

Figure 26: (Left) Ash plume from WRF-Chem subsampled on the CAIRT retrieval grid and corresponding CAIRT cloud extension retrieval (red rectangles). (Right) Ash density determined using SEVERI and CAIRT measurements.

7 Task 10: Community engagement and outreach

7.1 Users survey

A user survey was setup online to collect feedback from a diverse pool of users on applications and potential use of CAIRT products. The responses were a good sample of the range of applications that CAIRT products would enable, not only for scientific research but also for operational weather forecasting and policy-making.

The support CAIRT obtained from users and researchers from the U.S. was also noteworthy, which highlights the urgent need for a mission like CAIRT to provide observations of the whole atmosphere now that previous limb-imagers like MLS will stop functioning, and the unlike support for climate related satellite missions under the current U.S. Administration. CAIRT therefore also represented a unique opportunity to advance European leadership in Earth's Climate Observations, fulfilling a potential void in publicly available observing data of the whole atmosphere. The community expressed concern that without CAIRT, climate related questions that can be explored with limb observations are at risk of slowing down or cessation, putting at risk past investments in the field and sending climate and atmospheric research backwards in time.

7.2 Community engagement

To complement and expand our dissemination activities along Phase A, active engagement between the CAIRT Team and the wider scientific community was established through our collaboration networks and during conferences and networking events we attended. Strong support for CAIRT was explicitly expressed also from a number of international programmes and activities, with especial interest from WCRP activities like the Earth System Models and Observations (ESMO) and the APARC, for which observations of chemical and dynamical variables as planned for the CAIRT mission are essential. Interest from operational weather centres, Copernicus services and major reanalysis centres was also stated.

All this showed a large international community that would guarantee that CAIRT's observations are rapidly and effectively used for scientific, operational and societal applications.

7.3 Dissemination and Communication

7.3.1 Scientific Conferences

Results from studies conducted during Phase A, and relevance of CAIRT observations for climate and weather-related research have been presented by the CAIRT team at national and international conferences and workshops.

7.3.2 Scientific manuscripts and Special Issue

A joint Special Issue (Collection) is being setup with the Atmospheric Chemistry and Physics (ACP) journal and other relevant open-access EGU journals. More than 15 papers are already in preparation, or recently submitted, as a direct result of the work carried out by the PerReC activity during Phase A.

7.3.3 Communication and outreach events

Several outputs for general audiences and the media were also produced during Phase A of the PerReC activity and workshop events and sessions were organised with CAIRT content.

Full details about our communication, dissemination and outreach activities can be found in the dedicated deliverable DEL-22-CAIRT-PhAPerReC.

8 Outlook and Science Roadmap

The PerReC Phase A activities provided a comprehensive performance assessment and a demonstration of science closure for CAIRT's primary Mission Objectives, including some impact assessment for further science applications. A Science Roadmap for Phase B1 and beyond was compiled by PerReC. This roadmap sketches out activities for reaching the Science Readiness Levels required for implementation of the CAIRT mission. Many of these recommended future activities and studies would also be very relevant for advancing alternative infrared limb imaging approaches beyond EE11-CAIRT.

8.1 End-to-end simulator developments

The CAIRT End-to-end Performance Simulator CEEPS has been developed and tested during Phases 0 and A. All future activities towards infrared limb imaging tomography – including investigation of new and smaller instrument concepts and recommended further impact assessments – would greatly benefit from continued developments towards a versatile end-to-end simulator, capable to provide simulated observations and comprehensive error estimates for a range of possible instrument concepts. Future developments of the end-to-end simulator should work towards a confluence of Scientific Workbench (SWB and CEEPS).

8.2 Spectroscopy studies

Investigation of spectroscopic data and in particular spectroscopic uncertainties should be performed. This may include lab studies to better characterize spectroscopy in critical regions. Uncertainties of spectroscopic parameters are not well specified in most cases, limiting the ability to derive robust total uncertainty estimates of retrieved L2 parameters.

8.3 Level-2 prototype processor development

A particular challenge is the development of a fast processor to work under real-time conditions, capable of tomographic retrievals, as well as accurate representation of non-LTE effects. These activities should include specification, coding and testing of the prototype processor. Upcoming AI methods, including machine learning and physics-informed neural networks, present new opportunities to address the vast data volumes

of CAIRT, such as new avenues for retrieving the full range of target parameters as well as additional ones, for full 3D retrievals, direct L1b radiance assimilation, and more.

8.4 Data assimilation impacts/benefits studies

In addition to CAIRT's science goals, that remain valid and timely, there is a need for monitoring of the middle atmosphere, as well as a great potential for operational use of infrared limb imaging observations. Emerging threats and challenges of the middle atmosphere include the atmospheric impact of a strongly growing number of rocket-launches and satellite re-entry under upcoming mega-constellations as well as an increased likelihood of geoengineering (solar-radiation management) through the deliberate injection of aerosol particles into the stratosphere. These topics are currently assessed as part of the Montreal Protocol process for safeguarding of the ozone layer. Any upcoming European or international regulation requires monitoring of the middle atmosphere for compliance verification, but critically also for a better understanding of any adverse effects. Independent of this, there are strong indications, that operational use of limb observations can lead to significant improvements in numerical weather forecasting. Therefore, quantification of the impact of infrared limb observations on numerical weather prediction operational systems is strongly needed. Future studies should be performed to demonstrate and quantify the impact of infrared limb imaging on weather prediction as well as the potential to detect and attribute the atmospheric effects of geoengineering and satellite re-entry. These studies should ideally include relevant stakeholders and may include an assessment of socio-economic benefits of infrared limb imaging.

The efficient use of CAIRT data in applications requires developments towards data assimilation. Assimilation of L1 data (radiances) instead of L2 data offers a number of potential benefits: it is potentially more time efficient for near-real-time assimilation (avoiding the retrieval of L2 data first) and may avoid biases introduced during the retrieval process through additional assumptions on priors or regularization. To enable L1 assimilation, fast forward models suitable for integration in the NWP framework need to be developed, implemented, tested, and validated. A rapidly evolving field is the use of AI/Machine Learning methods to derive products (in particular weather forecasts in the NWP context) directly from L1 satellite observations. These methods should be investigated and developed for the use of CAIRT data.

References

Allen, A., Markou, S., Tebbutt, W., Requeima, J., Bruinsma, W.P., Andersson, T.R., Herzog, M., Lane, N.D., Chantry, M., Hosking, J.S., Turner, R.E., 2025. End-to-end data-driven weather prediction. Nature. https://doi.org/10.1038/s41586-025-08897-0

Añel, J.A., Cnossen, I., Antuña-Marrero, J.C., Beig, G., Brown, M.K., Doornbos, E., Osprey, S., Mutschler, S.M., Souto, C.P., Šácha, P., Sofieva, V., Torre, L.D.L., Zhang, S., Mlynczak, M.G., 2025. The Need for Better Monitoring of Climate Change in the Middle and Upper Atmosphere. AGU Adv. 6, e2024AV001465. https://doi.org/10.1029/2024AV001465

Castelli, E., Dinelli, B.M., Carlotti, M., Arnone, E., Papandrea, E., Ridolfi, M., 2011. Retrieving cloud geometrical extents from MIPAS/ENVISAT measurements with a 2-D tomographic approach. Opt. Express 19, 20704–20721. https://doi.org/10.1364/OE.19.020704

Ceccherini, S., Carli, B., Raspollini, P., 2015. Equivalence of data fusion and simultaneous retrieval. Opt. Express 23, 8476. https://doi.org/10.1364/OE.23.008476

Chabrillat, S., Vigouroux, C., Christophe, Y., Engel, A., Errera, Q., Minganti, D., Monge-Sanz, B.M., Segers, A., Mahieu, E., 2018. Comparison of mean age of air in five reanalyses using the BASCOE transport model. Atmos Chem Phys 18, 14715–14735. https://doi.org/10.5194/acp-18-14715-2018

Charlesworth, E., Plöger, F., Birner, T., Baikhadzhaev, R., Abalos, M., Abraham, N.L., Akiyoshi, H., Bekki, S., Dennison, F., Jöckel, P., Keeble, J., Kinnison, D., Morgenstern, O., Plummer, D., Rozanov, E., Strode, S., Zeng, G., Egorova, T., Riese, M., 2023. Stratospheric water vapor affecting atmospheric circulation. Nat. Commun. 14, 3925. https://doi.org/10.1038/s41467-023-39559-2

Engel, A., Bönisch, H., Ullrich, M., Sitals, R., Membrive, O., Danis, F., Crevoisier, C., 2017. Mean age of stratospheric air derived from AirCore observations. Atmospheric Chem. Phys. 17, 6825–6838. https://doi.org/10.5194/acp-17-6825-2017

Errera, Q., 2023. Extended reference scenarios (ERS) file (including only the temperature and trace species climatology). https://doi.org/10.5281/zenodo.10022129

Errera, Q., Dekemper, E., Baker, N., Debosscher, J., Demoulin, P., Mateshvili, N., Pieroux, D., Vanhellemont, F., Fussen, D., 2021. On the capability of the future ALTIUS ultraviolet–visible–near-infrared limb sounder to constrain modelled stratospheric ozone. Atmospheric Meas. Tech. 14, 4737–4753. https://doi.org/10.5194/amt-14-4737-2021

Errera, Q., Op De Beeck, M., Bender, S., Flemming, J., Funke, B., Hoffmann, A., Höpfner, M., Livesey, N., Poli, G., Pieroux, D., Raspollini, P., Sinnhuber, B.-M., 2025a. On the capability of the Changing Atmosphere Infra-Red Tomography explorer (CAIRT) candidate mission to constrain O_3 and H_2 O in the upper troposphere and lower stratosphere. https://doi.org/10.5194/egusphere-2025-6130

Errera, Q., Voet, F., Bender, S., Funke, B., Höpfner, M., Sinnhuber, B.-M., 2025b. DEL-15-1-CAIRT Case / Impact Study 1 for AoA (No. DEL-15-1-TR-2.1-CAIRT-PhAPerReC).

ESA Earth and Mission Science Division, 2025. CHANGING ATMOSPHERE INFRARED TOMOGRAPHY EXPLORER (CAIRT) MISSION REQUIREMENTS DOCUMENT (No. ESA-EOPSM-CAIR-MRD-4662, issue 0, revision 4).

Farchi, A., Chrust, M., Bocquet, M., Bonavita, M., 2024. Online model error correction with neural networks: application to the Integrated Forecasting System. https://doi.org/10.48550/arXiv.2403.03702

Forbes, L., Jarvis, D., Potts, J., Baxter, P.J., 2003. Volcanic ash and respiratory symptoms in children on the island of Montserrat, British West Indies. Occup. Environ. Med. 60, 207–211. https://doi.org/10.1136/oem.60.3.207

Fromm, M., Kablick III, G., Nedoluha, G., Carboni, E., Grainger, R., Campbell, J., Lewis, J., 2014. Correcting the record of volcanic stratospheric aerosol impact: Nabro and Sarychev Peak. J. Geophys. Res. Atmospheres 119, 10,343-10,364. https://doi.org/10.1002/2014JD021507

Garny, H., Ploeger, F., Abalos, M., Bönisch, H., Castillo, A.E., Von Clarmann, T., Diallo, M., Engel, A., Laube, J.C., Linz, M., Neu, J.L., Podglajen, A., Ray, E., Rivoire, L., Saunders, L.N., Stiller, G., Voet, F., Wagenhäuser, T., Walker, K.A., 2024. Age of Stratospheric Air: Progress on Processes, Observations, and Long-Term Trends. Rev. Geophys. 62, e2023RG000832. https://doi.org/10.1029/2023RG000832

Grell, G.A., Peckham, S.E., Schmitz, R., McKeen, S.A., Frost, G., Skamarock, W.C., Eder, B., 2005. Fully coupled “online” chemistry within the WRF model. Atmos. Environ. 39, 6957–6975. https://doi.org/10.1016/j.atmosenv.2005.04.027

Griessbach, S., Hoffmann, L., Spang, R., Riese, M., 2014. Volcanic ash detection with infrared limb sounding: MIPAS observations and radiative transfer simulations. Atmospheric Meas. Tech. 7, 1487–1507. https://doi.org/10.5194/amt-7-1487-2014

Guerrieri, L., Merucci, L., Corradini, S., Pugnaghi, S., 2015. Evolution of the 2011 Mt. Etna ash and SO2 lava fountain episodes using SEVIRI data and VPR retrieval approach. J. Volcanol. Geotherm. Res. 291, 63–71. https://doi.org/10.1016/j.jvolgeores.2014.12.016

Hogan, R.J., Ahlgrimm, M., Balsamo, G., Beljaars, A., Berrisford, P., Bozzo, A., Di Guiseppe, F., Forbes, R., Haiden, T., Lang, S., Mayer, M., Polichtchouk, I., Sandu, I., Vitart, F., Wedi, N., 2017. Radiation in numerical weather prediction (Technical memorandum No. 816), ECMWF Technical Memoranda. ECMWF, Reading.

Lawrence, Z.D., Abalos, M., Ayarzagüena, B., Barriopedro, D., Butler, A.H., Calvo, N., De La Cámara, A., Charlton-Perez, A., Domeisen, D.I.V., Dunn-Sigouin, E., García-Serrano, J., Garfinkel, C.I., Hindley, N.P., Jia, L., Jucker, M., Karpechko, A.Y., Kim, H., Lang, A.L., Lee, S.H., Lin, P., Osman, M., Palmeiro, F.M., Perlwitz, J., Polichtchouk, I., Richter, J.H., Schwartz, C., Son, S.-W., Erner, I., Taguchi, M., Tyrrell, N.L., Wright, C.J., Wu, R.W.-Y., 2022. Quantifying stratospheric biases and identifying their potential sources in subseasonal forecast systems. Weather Clim. Dyn. 3, 977–1001. https://doi.org/10.5194/wcd-3-977-2022

López-Puertas, M., Funke, B., 2015. RADIATION TRANSFER IN THE ATMOSPHERE | Non-Local Thermodynamic Equilibrium, in: North, G.R., Pyle, J., Zhang, F. (Eds.), Encyclopedia of Atmospheric Sciences (Second Edition). Academic Press, Oxford, pp. 16–26. https://doi.org/10.1016/B978-0-12-382225-3.00339-X

Masiello, G., Serio, C., Maestri, T., Martinazzo, M., Masin, F., Liuzzi, G., Venafra, S., 2024. The new σ-IASI code for all sky radiative transfer calculations in the spectral range 10 to 2760 cm-1: σ-IASI/F2N. J. Quant. Spectrosc. Radiat. Transf. 312, 108814. https://doi.org/10.1016/j.jqsrt.2023.108814

McNally, A., Lessig, C., Lean, P., Boucher, E., Alexe, M., Pinnington, E., Chantry, M., Lang, S., Burrows, C., Chrust, M., Pinault, F., Villeneuve, E., Bormann, N., Healy, S., 2024. Data driven weather forecasts trained and initialised directly from observations. https://doi.org/10.48550/ARXIV.2407.15586

Mlynczak, M.G., Yue, J., McCormack, J.P., Lieberman, R.S., Livesey, N.J., 2021. An Observational Gap at the Edge of Space. Eos.

Monge-Sanz, B.M., Bozzo, A., Byrne, N., Chipperfield, M.P., Diamantakis, M., Flemming, J., Gray, L.J., Hogan, R.J., Jones, L., Magnusson, L., Polichtchouk, I., Shepherd, T.G., Wedi, N., Weisheimer, A., 2022. A stratospheric prognostic ozone for seamless Earth system models: performance, impacts and future. Atmospheric Chem. Phys. 22, 4277–4302. https://doi.org/10.5194/acp-22-4277-2022

O'Neill, B.C., Tebaldi, C., Van Vuuren, D.P., Eyring, V., Friedlingstein, P., Hurtt, G., Knutti, R., Kriegler, E., Lamarque, J.-F., Lowe, J., Meehl, G.A., Moss, R., Riahi, K., Sanderson, B.M., 2016. The Scenario Model Intercomparison Project (ScenarioMIP) for CMIP6. Geosci. Model Dev. 9, 3461–3482. https://doi.org/10.5194/gmd-9-3461-2016

Plane, J.M.C., Gumbel, J., Kalogerakis, K.S., Marsh, D.R., von Savigny, C., 2023. Opinion: Recent developments and future directions in studying the mesosphere and lower thermosphere. Atmospheric Chem. Phys. 23, 13255–13282. https://doi.org/10.5194/acp-23-13255-2023

Ploeger, F., Legras, B., Charlesworth, E., Yan, X., Diallo, M., Konopka, P., Birner, T., Tao, M., Engel, A., Riese, M., 2019. How robust are stratospheric age of air trends from different reanalyses? Atmospheric Chem. Phys. 19, 6085–6105. https://doi.org/10.5194/acp-19-6085-2019

Prata, A.J., Tupper, A., 2009. Aviation hazards from volcanoes: the state of the science. Nat. Hazards 51, 239–244. https://doi.org/10.1007/s11069-009-9415-y

Rhode, S., 2025. Identifying Orographic Gravity Waves in 3D Observations via Backward Ray Tracing. https://doi.org/10.5194/egusphere-2025-4946

Rhode, S., Preusse, P., Ungermann, J., Polichtchouk, I., Sato, K., Watanabe, S., Ern, M., Nogai, K., Sinnhuber, B.-M., Riese, M., 2024. Global-scale gravity wave analysis methodology for the ESA Earth Explorer 11 candidate CAIRT. Atmospheric Meas. Tech. 17, 5785–5819. https://doi.org/10.5194/amt-17-5785-2024

Riese, M., Ploeger, F., Rap, A., Vogel, B., Konopka, P., Dameris, M., Forster, P., 2012. Impact of uncertainties in atmospheric mixing on simulated UTLS composition and related radiative effects. J. Geophys. Res. Atmospheres 117, n/a-n/a. https://doi.org/10.1029/2012JD017751

Robock, A., 2013. The Latest on Volcanic Eruptions and Climate. Eos Trans. Am. Geophys. Union 94, 305–306. https://doi.org/10.1002/2013EO350001

Robock, A., 2010. New START, Eyjafjallajökull, and Nuclear Winter. Eos Trans. Am. Geophys. Union 91, 444–445. https://doi.org/10.1029/2010EO470004

Robock, A., 2000. Volcanic eruptions and climate. Rev. Geophys. 38, 191–219. https://doi.org/10.1029/1998RG000054

Rodgers, C.D., 2000. Inverse methods for atmospheric sounding: theory and practice, Series on atmospheric, oceanic and planetary physics. World Scientific, Singapore.

Salawitch, R.J., Smith, J.B., Selkirk, H., Wargan, K., Chipperfield, M.P., Hossaini, R., Levelt, P.F., Livesey, N.J., McBride, L.A., Millán, L.F., Moyer, E., Santee, M.L., Schoeberl, M.R., Solomon, S., Stone, K.,

Worden, H.M., 2025. The Imminent Data Desert: The Future of Stratospheric Monitoring in a Rapidly Changing World. Bull. Am. Meteorol. Soc. https://doi.org/10.1175/BAMS-D-23-0281.1

Scaife, A.A., Baldwin, M.P., Butler, A.H., Charlton-Perez, A.J., Domeisen, D.I.V., Garfinkel, C.I., Hardiman, S.C., Haynes, P., Karpechko, A.Y., Lim, E.-P., Noguchi, S., Perlwitz, J., Polvani, L., Richter, J.H., Scinocca, J., Sigmond, M., Shepherd, T.G., Son, S.-W., Thompson, D.W.J., 2022. Long-range prediction and the stratosphere. Atmospheric Chem. Phys. 22, 2601–2623. https://doi.org/10.5194/acp-22-2601-2022

Scaife, A.A., Karpechko, A.Yu., Baldwin, M.P., Brookshaw, A., Butler, A.H., Eade, R., Gordon, M., MacLachlan, C., Martin, N., Dunstone, N., Smith, D., 2016. Seasonal winter forecasts and the stratosphere. Atmospheric Sci. Lett. 17, 51–56. https://doi.org/10.1002/asl.598

Schoenhardt, A., Arola, A., Benedictow, A., Bennouna, Y., Bouarar, I., Cuevas, E., Errera, Q., Eskes, H.J., Griesfeller, J., Ilic, L., Kapsomenakis, J., Langerock, L., Mortier, A., Pison, I., Pitkänen, M.R.A., Ramonet, M., Richter, A., Schulz, M., Tarniewicz, J., Thouret, V., Tsikerdekis, A., Warneke, T., A. A. Zerefos, 2023. Validation report of the CAMS near-real-time global atmospheric composition service, Period September - November 2022 (No. doi:10.24380/rrmj-aj0k).

Semane, N., Bonavita, M., 2025. Reintroducing the analysis of humidity in the stratosphere. ECMWF Newsl.

Stuefer, M., Freitas, S.R., Grell, G., Webley, P., Peckham, S., McKeen, S.A., Egan, S.D., 2013. Inclusion of ash and SO_2 emissions from volcanic eruptions in WRF-Chem: development and some applications. Geosci. Model Dev. 6, 457–468. https://doi.org/10.5194/gmd-6-457-2013

Tilmes, S., MacMartin, D.G., Lenaerts, J.T.M., Van Kampenhout, L., Muntjewerf, L., Xia, L., Harrison, C.S., Krumhardt, K.M., Mills, M.J., Kravitz, B., Robock, A., 2020. Reaching 1.5 and 2.0 °C global surface temperature targets using stratospheric aerosol geoengineering. Earth Syst. Dyn. 11, 579–601. https://doi.org/10.5194/esd-11-579-2020

Tirelli, C., Ceccherini, S., Del Bianco, S., Funke, B., Höpfner, M., Cortesi, U., Raspollini, P., 2025. Extension of the Complete Data Fusion algorithm to tomographic retrieval products. EGUsphere 1–24. https://doi.org/10.5194/egusphere-2025-1283

Vervalcke, S., Errera, Q., Eichinger, R., Reddmann, T., Chabrillat, S., Op De Beeck, M., Stiller, G., Mahieu, E., 2026. Atmospheric lifetime of sulphur hexafluoride (SF_6) and five other trace gases in the BASCOE model driven by three reanalyses. Atmospheric Chem. Phys. 26, 391–409. https://doi.org/10.5194/acp-26-391-2026

Voet, F., Ploeger, F., Laube, J., Preusse, P., Konopka, P., Grooß, J.-U., Ungermann, J., Sinnhuber, B.-M., Höpfner, M., Funke, B., Wetzel, G., Johansson, S., Stiller, G., Ray, E., Hegglin, M.I., 2025. On the estimation of stratospheric age of air from correlations of multiple trace gases. Atmospheric Chem. Phys. 25, 3541–3565. https://doi.org/10.5194/acp-25-3541-2025

von Clarmann, T., Degenstein, D.A., Livesey, N.J., Bender, S., Braverman, A., Butz, A., Compernolle, S., Damadeo, R., Dueck, S., Eriksson, P., Funke, B., Johnson, M.C., Kasai, Y., Keppens, A., Kleinert, A., Kramarova, N.A., Laeng, A., Langerock, B., Payne, V.H., Rozanov, A., Sato, T.O., Schneider, M., Sheese, P., Sofieva, V., Stiller, G.P., von Savigny, C., Zawada, D., 2020. Overview: Estimating and reporting uncertainties in remotely sensed atmospheric composition and temperature. Atmospheric Meas. Tech. 13, 4393–4436. https://doi.org/10.5194/amt-13-4393-2020

von Clarmann, T., Glatthor, N., Grabowski, U., Funke, B., Kiefer, M., Kleinert, A., Stiller, G.P., Linden, A., Kellmann, S., 2022. TUNER-compliant error estimation for MIPAS: methodology. Atmospheric Meas. Tech. 15, 6991–7018. https://doi.org/10.5194/amt-15-6991-2022

WMO, NOAA, UNEP, NASA, European Commission, 2023. GAW Report - 278. Scientific Assessment of Ozone Depletion: 2022 (No. 278), GAW Report. WMO, Geneva.

WMO, UNEP, ISC, IOC-UNESCO, 2022. The 2022 GCOS Implementation Plan (GCOS-244) (No. GCOS-244). WMO, Geneva, Switzerland.

Zehner, C., 2010. Monitoring Volcanic Ash from Space, in: Monitoring Volcanic Ash from Space. Presented at the ESA-EUMETSAT workshop on the 14 April to 23 May 2010 eruption at the Eyjafjoll volcano, South Iceland, ESA - STM-280. https://doi.org/10.5270/atmch-10-01

Appendix: List of deliverables

Deliverable ID (Study)	Ref number	Title	Final version	Publically available
DEL-03 (PerReC)	DEL-03-CAIRT-PhAPerReC-1.3	Scientific applications, end-user, and observation requirements for the CAIRT mission	23.01.2026	Y
DEL-04-01a (PerReC)	DEL-04-01a-ATBD-CAIRT-PhAPerReC-2.1	CAIRT linear SWB ATBD	20.11.2025	Y
DEL-04-01b (PerReC)	DEL-04-01b-ATBD CAIRT-PhAPerReC-1.1	CAIRT JURASSIC2 ATBD	26.09.2025	Y
DEL-04-01c (PerReC)	DEL-04-01c-ATBD CAIRT-PhAPerReC-1.2	CAIRT Level 2 ATBD	01.10.2025	Y
DEL-04-01d (PerReC)	DEL-04-01d-ATBD-CAIRT-PhAPerReC-1.0	ATBD-KOPRA	14.10.2024	Y
DEL-04-02 (PerReC)	DEL-04-02-ATBD CAIRT-PhAPerReC-1.1	Algorithm Theoretical Basis Document for CAIRT product L2b overview	16.09.2025	Y
DEL-04-03a (PerReC)	DEL-04-03a CAIRT-PhAPerReC-2.1	Core of technical paper on GWBG removal	06.11.2025	Y
DEL-04-03b (PerReC)	D-04-03b-CAIRT-PhAPerReC-2.0	GWBG Core of technical paper on GW	19.01.2026	Y
DEL-04-03c (PerReC)	DEL-04-03c-CAIRT-PhAPerReC-2.0	Core of technical paper on AoA - On the estimation of stratospheric age of air from correlations of multiple trace gases	02.07.2025	Y
DEL-05 (PerReC)	DEL-05-CAIRT-PhAPerReC-v3.1	PSD: “CAIRT L2(+) Product Specification Document”	01.12.2025	Y
DEL-06 (PerReC)	DEL-06-CAIRT-PhAPerReC-1.1	Product Validation Plan	23.10.2025	Y
DEL-07 (PerReC)	DEL-07-CAIRT-PhAPerReC-2.0	CAIRT Mission Performance Evaluation Plan (MPEP)	08.09.2025	N
DEL-08 (PerReC)	DEL-08-TN2-CAIRT-PhAPerReC-v1.3	CAIRT Test Data Sets for Mission Performance Evaluation -Technical Note TN-2	19.11.2025	N
DEL-09 (PerReC)	DEL-09-CAIRT-PhAPerReC-v3.1	CAIRT measurement requirements assessment -Technical Note TN-3	19.11.2025	Partly
DEL-09.1 (PerReC)	DEL-09.1-CAIRT-PhAPerReC-v6.0	Technical note on Yaw-steering for CAIRT	10.10.2025	Y
DEL-09.2 (PerReC)	DEL-09.2-CAIRT-PhAPerReC-v5.0	Technical note on pointing jitter	04.03.2024	Y
DEL-09.3 (PerReC)	DEL-09.3-CAIRT-PhAPerReC-v3.0	Technical note on spectral calibration	21.10.2024	Y
DEL-09.4 (PerReC)	DEL-09.4-CAIRT-PhAPerReC-v5.0	Technical note on diffraction/far field SEDF	10.10.2025	Y
DEL-09.5 (PerReC)	DEL-09.5-CAIRT-PhAPerReC-1.0	Technical note on L2 performance for FOV widths 1.4 km vs 1.5 km	11.10.2024	Y
DEL-09.6 (PerReC)	DEL-09.6-CAIRT-PhAPerReC-6.0	Technical note on SEDF requirement	09.10.2025	Y
DEL-09.7 (PerReC)	DEL-09.7-CAIRT-PhAPerReC-1.0	Technical note on horizontal vs. vertical atmospheric variability	16.08.2024	Y

DEL-09.8 (PerReC)	DEL-09.8-CAIRT-PhAPerReC-2.0	Technical note analog-digital discretization error	10.10.2025	Y
DEL-09.9 (PerReC)	DEL-09.9-CAIRT-PhAPerReC-1.1	Technical Note: Influence of calibration gaps and dead subsamples	08.10.2025	Y
DEL-09-10	DEL-09.10-CAIRT-PhAPerReC-1.0	Technical note on cloud influence	22.09.2025	Y
DEL-10 (PerReC)	DEL-10-CAIRT-PhAPerReC-v2.1	Evaluation of CAIRT scientific performance in Phase A through analysis and demonstration - Technical Report TR-1	19.11.2025	Partly
DEL-10-2 (PerReC)	DEL-10.2-CAIRT-PhAPerReC-1.1	Uncertainty estimation of gravity wave parameters by Monte Carlo Simulation	14.01.2026	Y
DEL-12 (PerReC)	DEL-12-CAIRT-PhAPerReC-2.0	Scientific and societal relevance and impact studies for the CAIRT mission	02.10.2025	Y
DEL-13 (PerReC)	DEL-13-CAIRT-PhAPerReC-1.0	CAIRT Mission Impact Assessment Plan - MIAP	17.10.2024	N
DEL-14-1(PerReC)	DEL-14-1-CAIRT-PhAPerReC-1.0	Readme-1: CAIRT mission test data set product descriptions for impact study on Age of Air	19.09.2025	Y
DEL-14-2 (PerReC)	DEL-14-2-CAIRT-PhAPerReC-3.0	Readme-2: CAIRT mission product test data set descriptions for case/impact studies for Consistent simulation of GW and MLT	16.01.2026	Y
DEL-14-3 (PerReC)	DEL-14-3-CAIRT-PhAPerReC-2.0	Readme-3: CAIRT mission product test data set descriptions for case/impact studies for geoengineering	18.11.2025	Y
DEL-14-4 (PerReC)	DEL-14-4-CAIRT-PhAPerReC-2.0	Readme-4: CAIRT mission product test data set descriptions for case/impact studies UTLS O3 OSSE	19.09.2025	Y
DEL-14-5 (PerReC)	DEL-14-5-CAIRT-PhAPerReC-1.1	Readme-5: CAIRT mission product test data set descriptions for impact study Stratosphere/UTLS and weather and climate predictability	23.01.2026	Y
DEL-14-6 (PerReC)	DEL-14-6-CAIRT-PhAPerReC-2.0	Readme-6: CAIRT mission product test data set descriptions for case/impact studies for volcanic ash detection	26.09.2025	Y
DEL-15-1 (PerReC)	DEL-15-1-TR2.1-CAIRT-PhAPerReC-1.0	CAIRT Case / Impact Study 1 for AoA	17.10.2025	Y
DEL-15-2 (PerReC)	DEL-15-2-TR2.2-CAIRT-PhAPerReC-1.1	CAIRT Case / Impact Study 2 for consistent simulation of GW and MLT	29.09.2025	Y
DEL-15-3 (PerReC)	DEL-15-3-TR2.3-CAIRT-PhAPerReC-3.0	CAIRT Case / Impact Study 3 Geoengineering via Stratospheric Sulfur Injection	30.09.2025	Y
DEL-15-4 (PerReC)	DEL-15-TR2.4-CAIRT-PhAPerReC-1.1	CAIRT Case / Impact Study 4 for UTLS O3 OSSE	14.01.2026	Y
DEL-15-5 (PerReC)	DEL-15-TR2.5-CAIRT-PhAPerReC-1.0	CAIRT Case / Impact Study 5 for Stratosphere/UTLS and weather and climate prediction	23.01.2026	Y
DEL-15-6 (PerReC)	DEL-15-TR2.6-CAIRT-PhAPerReC-2.0	CAIRT Case / Impact Study 6 for volcanic ash	03.07.2025	Y

DEL-16 (PerReC)	DEL-16-CAIRT-PhAPerReC-2.3	CAIRT bibliographic reference list	22.01.2026	Y
DEL-18 (PerReC)	DEL-18-CAIRT-PhAPerReC-1.0	SRM: "Scientific roadmap for CAIRT beyond Phase A/B1"	15.10.2025	N
DEL-19 (PerReC)	D-19-TR3/FR:	Consolidated inputs for the CAIRT Report for Mission Selection	20.01.2026	N RfMS->Y
DEL-21 (PerReC)	DEL-21-CAIRT-PhAPerReC-1.1	Peer-reviewed publications (or manuscripts in review) based on CAIRT scientific work	20.01.2026	N
DEL-22 (PerReC)	DEL-22-CAIRT-PhAPerReC-1.2	Record of dissemination and outreach activities	20.01.2026	N
DEL-24 (PerReC)	DEL-24-CAIRT-PhAPerReC-1.2	Executive Summary Report	22.01.2026	Y
DEL-25 (PerReC)	DEL-25-CAIRT- PhAPerReC	Contract Closure Documentation	23.01.2026	N
DEL- DATA-SW-LIB-WEB (PerReC)	DEL- DATA-SW-LIB-WEB-CAIRT- PhAPerReC-1.4	DATA-01, DATA-02, DATA-03, LIB-01, LIB-02, LIB-03, SW-01, WEB-01	11.12.2025	Y

CAIRT study documents marked "Y" will be accessible via Zenodo public repository, and will be findable via https://zenodo.org/communities/cairt-scirec/records site (https://doi.org/10.5281/zenodo.18496134).